REPUBLIC OF TURKEY

GAZİANTEP UNIVERSITY

GRADUATE SCHOOL OF NATURAL & APPLIED SCIENCES

BANDWIDTH AND GAIN ENHANCEMENT OF MICROSTRIP ANTENNA USING METAMATERIALS

M. Sc. THESIS

IN

ELECTRICAL AND ELECTRONICS ENGINEERING

BY

ALI FARAJ DARWEESH

JUNE 2019

Bandwidth And Gain Enhancement Of Microstrip Antenna Using Metamaterials

M.Sc. Thesis

in

Electrical and Electronics Engineering

Gaziantep University

Supervisor

Prof. Dr. Gölge ÖGÜCÜ YETKIN

by

Ali Faraj Darweesh

June 2019

I hereby declare that all information in this document has been obtained and presented in accordance with academic rules and ethical conduct. I also declare that, as required by these rules and conduct, I have fully cited and referenced all material and results that are not original to this work.

Ali Faraj DARWEESH

ABSTRACT

BANDWIDTH AND GAIN ENHANCEMENT OF MICROSTRIP ANTENNA USING METAMATERIALS

DARWEESH, Ali Faraj
M.Sc. in Electrical and Electronics Engineering
Supervisor: Prof. Dr. Gölge ÖGÜCÜ YETKİN
June 2019
69 pages

In this thesis, the design of the ultra-wideband microstrip antenna based on a metamaterial (MTM) array is presented to increase antenna performance by enhancing the bandwidth and gain. The proposed structure consists of an ultra-wideband antenna and a metamaterial array. The design consists of three steps. In the first step, a traditional microstrip antenna of dimensions 36 x 38 mm^2 printed on FR4-Epoxy dielectric substrate with 1.58 mm thickness has been presented. In the second step, a partial ground plane technique has been applied on microstrip patch antenna with the transition steps. A UWB antenna has been obtained that is operating between 2.6 GHz and more than 20 GHz. In the third step, two unit cells of MTMs have been added on the microstrip antenna with a partial ground plane in order to increase the gain of the antenna about 3.19 dB.

Keywords Gain, Bandwidth, Ultra Wideband Antenna, Metamaterial

ÖZET

MİKROŞERİT ANTENININ METAMALZEMELER KULLANILARAK BANT GENİŞLİĞİ VE KAZANCININ ARTIRILMASI

DARWEESH, Ali Faraj
Yüksek Lisans Tezi, Elektrik-Elektronik Müh.
Tez Yöneticisi: Prof. Dr. Gölge ÖGÜCÜ YETKİN
Haziran 2019
69 sayfa

Bu tezde, bir meta malzeme (MTM) dizisine dayanan ultra geniş bantlı mikro şerit antenin tasarımı, bant genişliğini ve kazancını artırarak anten performansını artırmak için sunulmuştur. Önerilen yapı, ultra geniş bantlı bir anten ve bir meta malzeme dizisinden oluşur. Tasarım üç adımdan oluşuyor. İlk adımda, 1.58 mm kalınlığında FR4-Epoksi dielektrik substrat üzerine basılmış 36 x 38 mm2 boyutlarında geleneksel bir mikro şerit anten sunulmuştur. İkinci adımda, geçiş basamaklarıyla birlikte mikro şerit yama antenine kısmi bir yer düzlemi tekniği uygulanmıştır. 2,6 GHz ve 20 GHz'den daha fazla çalışan bir UWB anteni elde edildi. Üçüncü adımda, antenin kazancını yaklaşık 3.19 dB arttırmak için mikro hatlı antene kısmi bir toprak düzlemine sahip iki birim MTM hücresi eklenmiştir.

Anahtar Kelimeler: Kazanç, Bant Genişliği, Ultra Geniş Bant Anten, Metamalzeme.

To My Father……

I would like to dedicate this Master thesis to my father, he was the reference of my decisions and source of my strength throughout all the work stages and my life.

ACKNOWLEDGMENTS

I would like to express my deepest gratitude to my supervisor Prof.Dr. Gölge Ögücü Yetkin who gave me the golden opportunity to do this wonderful project on the Microstrip patch antenna Also,

Many thanks go to all my friends without any exception for the encouragement, patience and for being there for me when I needed. Thank you!

TABLE OF CONTENTS

Page

LIST OF TABLES

Page

LIST OF FIGURES

Page

LIST OF SYMBOLS

f	Frequency
f_r	Resonant Frequency
Q	Quality factor
λ	Wavelength
λ_o	Free space Wavelength
W	Transmission line width
t	Conductor thickness
C	Speed of Light
C_o	light velocity in free space
L	Patch length
L_{eff}	the effective length of Patch
E	Electric Field
H	Magnetic Field
μ	Permeability
ε	Permittivity
μ_r	Relative Permeability
ε_r	Relative Permittivity
$tan\ \delta$	Loss Tangent
n	Refraction Index
p	Unit Cell Size
h	Substrate Thickness
d	Separation distance

LIST OF ABBREVIATIONS

Acronym	Description
MCB	Microwave Circuit Board
MTM	Metamaterial
GHz	Giga-hertz
dB	Decibel
CST	Computer Simulation Technology
UWB	Ultra-Wideband
PTMA	Planar Triangular Monopole Antenna
mm	Millimeters
SHF	super high frequency
CPW	coplanar waveguide
DNM	Double Negative Metamaterial
FSS	Frequency Selective Surface
F/B	front-to-back
MIMO	Multi-Input-Multi-Output
PCB	printed-circuit board
GPS	Global positioning system

RFID	Radio frequency identification
WiMax	Worldwide interoperability for microwave access
RF	Radio Frequency
EMC	electromagnetically coupled
BW	Bandwidth
MoM	Method of Moments
FEM	Finite Element Method
FDTD	Finite Difference Time Domain
TLM	Transmission Line Matrix
FIT	Finite Integration Technique
PBA	Perfect Boundary Approximation
DPM	Double Positive Metamaterial
EBG	Electromagnetic Band Gap
ENG	Epsilon Negative
FEM	Finite Element Method
GBWP	Gain-Bandwidth Product
HFSS	High-Frequency Structure Simulator
MNG	Mu Negative
MSA	Microstrip Antenna
MTM	Metamaterial
PEC	Perfect Electric Conductor
PMC	Perfect Magnetic Conductor

SNG	Single Negative
SNG	Single Negative Metamaterial
SRR	Split Ring Resonator
TSRR	The triple Split Ring resonator
VSWR	Voltage Standing Wave Ratio
E-filed	Electric field
H-filed	Magnetic field

CHAPTER 1

INTRODUCTION AND LITERATURE SURVEY

1.1 Introduction

In continuous developments in the wireless communications industry, a need for antennas of exceptional capabilities has increased. A high gain with multiband/ wideband support antennas will be an ideal solution. Despite these challenges, antenna design specifications are scarcely relaxed, thus, it is generally difficult to achieve the desired antenna performance under these continuing developments in the wireless industry.

Microstrip patch antennas are characterized by many advantages such as slim profile, low production cost, lightweight, easy to fabricate and integrated with a microwave circuit board (MCB). However, the microstrip antennas also suffer from deep-rooted limitations such as narrow bandwidth, low efficiency, a modest gain, low ability to process energy, and strange radiation due to surface waves.

Many techniques were proposed to overcome conventional microstrip antennas limitations and for example, high-permittivity substrates, shorting posts, meanders, spirals, truncated patches, and lumped elements were proposed to reduce the antenna size. While a partial ground plane was proposed to overcome the bandwidth limitation. As shown from above, the size and the performance of antennas are usually commonly related in a different matrix; i.e., improving some characteristics may affect others. In the last few years, a novel way was proposed to overcome these limitations. This technique is presented by using various metamaterial (MTM) structures. A metamaterial is defined as an artificial material characterized (-μ and -ε) which the properties of metamaterial depend on the shape, orientation, arrangement, and size of the structure.

1.2 Problem Statement

The conventional microstrip antennas have many advantages such as slim profile, low production cost, lightweight, easy to fabricate and integrated with the circuit board. However, the disadvantages of microstrip antennas can be summarized as follows, narrow bandwidth, low efficiency, and modest gain. This work is an attempt to solve these problems by use of:

1- Transition steps with partial ground plane techniques to overcome the bandwidth limitation.
2- Metamaterial array to enhance the gain of the antenna.

1.3 Literature Survey

Many UWB antennas have been analyzed and presented in the literature in order to achieve the necessary for different applications. Gain enhancements and bandwidth developments are the most important requirements. As microstrip patch antennas ordinarily own narrow bandwidth features, it was there various methods developed for bandwidth improvement in order to produce UWB properties.

1.3.1 Microstrip Patch Antenna

Many designers have designed the antenna n different forms using specific methods to increase the interpretation of this antenna, for example, the rectangular microstrip patch antenna designed by it. iM. Luk *t al* based in L-shaped probe with foam substrate thickness around 10% of the wavelength. This antenna provides a bandwidth started from 3.76 GHz to 5.44 GHz and increased the gain equals to 7.5 dB [1], K.-S. Lim, [2] introduced a compact (UWB) microstrip antenna. The suggested antenna has a bandwidth from 4.1 GHz to 10 GHz. But this antenna has narrower bandwidth compared with the bandwidth allocated by federal communications commission FCC, which is from 3.1 GHz to 10.6 GHz. One of ithe methods used to upscale the bandwidth is ifound in [3]. They proposed that the antenna includes a rectangular patch powered by double steps, individual aperture above the patch and a partial ground plane as shown in Figure 1.1. The antenna operate the frequency range from 3.2 GHz to 12 iGHz is greater than that observed in [4] since it has a wider bandwidth and a more solid gain in the bandwidth range.

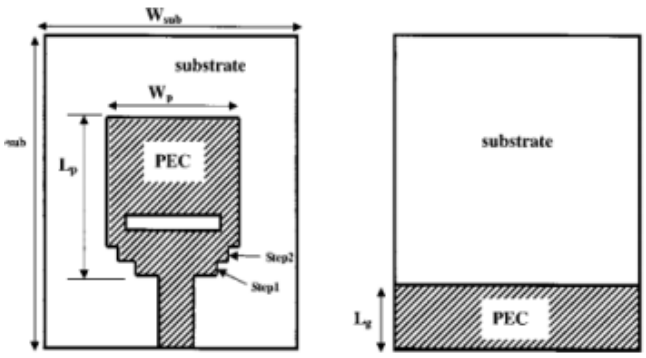

Figure 1.1 Patch, single aperture and partial ground plane [3].

Recently other mechanisms have been measured into magnify the bandwidth of UWB antenna including the addition of a modified shape of a short-tempered ground plane which is also having in thick profile and suitable to be printed with PCB. Tariqa it all [5] submitted a microstrip printed rectangular antenna structure which includes a patch with square shape iand a impartial ground back surface with multiplied is lots it top inside is shown in Figure 1.2.

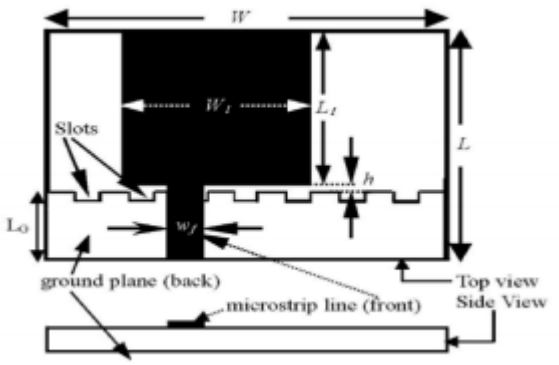

Figure 1.2 Partial ground plane technique with multiple rectangular slots at the top side [5].

Another method for expanding the impedance bandwidth of miniature antennas are found in [6], a rectangular planar antenna has the acting bandwidth extending from 3GHz to 8GHz by combining various technologies into one. By trimmed ground plane, and adding extra patch printed into the back side of the substrate, beneath the rectangular radiator as shown in Figure 1.3, the bandwidth can be distantly increased to cover wide bandwidth.

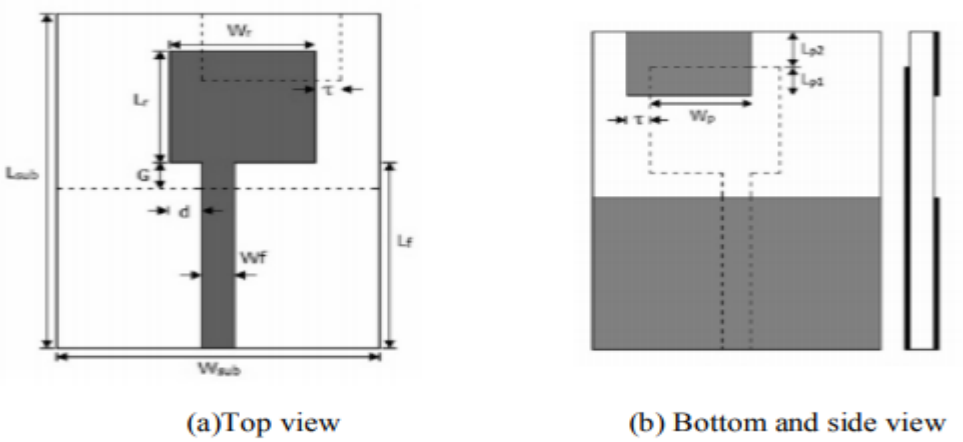

Figure 1.3. Antenna with an extra patch on substrate bottom (a)top view, (b) back and sides view.

A novel triangular fractal shaped patch antenna printed on an FR4-Epoxy substrate layer with a dimension of 40 x 40 x 1 mm^3. Such antenna gives a bandwidth in the range 4.33-8.54 GHz [7], A. A. Kalteh *et al.*, in 2014, a circular ring patch antenna with L shape ground plane printed on the FR4-Epoxy substrate with the dimension of 45 x 40 x 1.6 mm^3. Swapnil M. Vanam and Prof. R. P. Labade introduced a rectangular patch microstrip antenna that printed on an FR4-Epoxy substrate layer of dimension 33 x 25 mm^2. The bandwidth, $S_{11} \leq$ -10 dB, of such antenna is found to start from 3.1 GHz to 12 GHz [8].

1.3.2 UWB Microstrip Patch Antenna Based on Metamaterial

A novel SRR loaded to rectangular patch antenna by Sajith.K, the designed iSRR loaded more improper for monitoring of EEG and communications. The antenna has been intended with a followingdimension is 33 x 35 x 1.6 mm^3 the all suggested SRR loaded antenna has resonated it a resonance frequency range from 2.4 GHz to 2.45 GHz. The band (2.4 GHz to i2.5 GHz) antennas are also viable to advance the control mode of service in IMD and the design can be used permittivity which used for the substrate in this article is very high and affecting on bandwidth. In the future, if change the substrate from roger to FR-4 with $\varepsilon_r = 4.4$ and loss tangent 0.02 and print the partial ground plane on the bottom side of the substrate [9].

In 2015, Salhi *et al*. recommended an MTM refractive surface assimilated with coplanar wideband antenna, with the general antenna size being 50 x mm 40 mm. The MTM demonstrated a negative refractive index. The result showed improvement in the performance of the antenna [10]. In 2016, Kurra *et al*. conducted experiments to exhibit a uni-planar electromagnetic bandgap unit cell's FSS screen attributes. The unit cell consisted of a meander line inductor and, on one side of a substrate, inter-digital capacitors were present. As a superstrate for a specific distance in a patch antenna, the FSS screen was employed to improve antenna directivity. In addition, FSS structures offered high impedance surface that included a band stop or bandpass spectral behaviors based on the kind of array element. The result demonstrated in-phase image currents as well as decreased surface waves [11]. Based on the earlier work, it can be seen that including MTM along with antenna structures could result in improved performance of the wireless communication systems.

1.4 Aims of the Work

The aims of this research are to enhance the bandwidth and the gain of the microstrip antenna in order to obtain a UWB antenna.

The plan of this research can be summarized as follows:

1- Design a traditional microstrip patch antennas of inherent limitations; narrow bandwidth, low efficiency, and modest gain.
2- Design split-ring resonator structure.
3- Overcome the bandwidth limitations of the traditional antenna by applying transition steps and partial ground plane techniques.
4- Overcome the gain limitations of conventional microstrip antenna by combining the antenna designed with the SRR MTM array.

1.5 Thesis Organization

This thesis is consisting of five chapters that organized as follows:

Chapter One:

In this chapter, an overview of the thesis, Problem statement, literature review, aim of the work, and thesis outline are presented.

Chapter Two:

In this chapter, two structures are presented a microstrip antenna and metamaterials. The first part discusses the theory, properties, types of microstrip antennas, while the second part discusses the theory, properties, and types of the metamaterials (MTMs).

Chapter Three

This chapter presents the designing steps of the UWB microstrip patch antenna from the traditional one until arriving at the optimum design. The performances of such antenna are obtained in terms of return losses (S_{11}), Voltage standing wave ratio, gain, and the directivity, current distribution, 2D, and 3D radiation patterns.

Chapter Four:

In this chapter, the TSRR array is applied to the UWB antenna with studying the effects of such material on the antenna performance. Based on a parametric study, the best result is achieved in terms of return losses (S_{11}), Voltage standing wave ratio (VSWR), gain and the directivity, current distribution, 2D and 3D radiation patterns.

Chapter Five:

The conclusions and the suggestions for future work are presented

CHAPTER 2

THEORY OF MICROSTRIP ANTENNAS AND METAMATERIALS

2.1 Introduction

The first part of this chapter introduces some of the basic concepts of microstrip antennas. Three popular methods for the microstrip antennas analysis will be discussed transmission line model, cavity model, and full wave model are presented.

The second part of this chapter discusses the basic concepts of the metamaterials: History of the metamaterial starting from the first theory until the first experience that succeeded to achieve the metamaterial. Types of the metamaterials and the properties of each one are given next. Finally, the metamaterial applications and why it became widely used in microwave devices, especially in the antenna field are discussed.

matching antennas for rockets and spacecraft has begun to develop rapidly in microstrip antennas in the early 1970s. Some of this work is presented in advance [12]. Microstrip antennas can be classified according to their physical parameters and thus can be manufactured in different dimensions and shapes. Basic Microstrip antennas can be classified into microstrip dipoles, microstrip patch antennas, microstrip traveling wave antennas and printed slot antennas

2.2. Microstrip Patch Antenna

A microstrip patch antenna is the simplest form of microstrip antenna consisting of a radiating patch on the top side of a dielectric substrate and has a ground plane on the bottom side of the substrate is shown in Figure 2.1. Generally, conducting material like copper or gold are used to the patch and can take any possible shape. The feed line and patch are etched on the dielectric substrate. For a

rectangular patch, the patch thickness (t) is selected to be very thin such that $t << \lambda o$ where λo is the free-space wavelength. The patch width is usually $0.3333\ \lambda o < W < 0.5\ \lambda o$,. The height of the substrate is usually $0.003\ \lambda o \leq h \leq 0.05\ \lambda o$. The substrate dielectric constant (ε_r) is typically in the range of $2.2 \leq \varepsilon_r \leq 16$ [13].

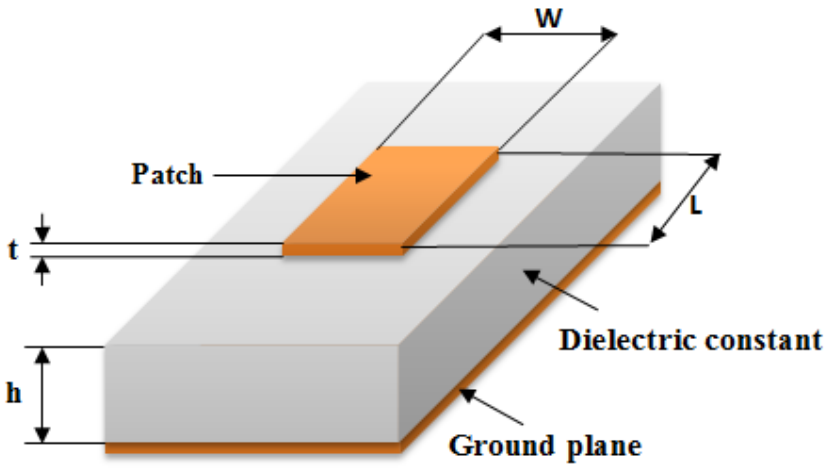

Figure 2.1 The basic structure of a microstrip patch antenna [14].

To simplify analysis and performance prediction, the patch is generally square, rectangular, circular, triangular and elliptical or some other common shapes is shown in Figure 2.2.

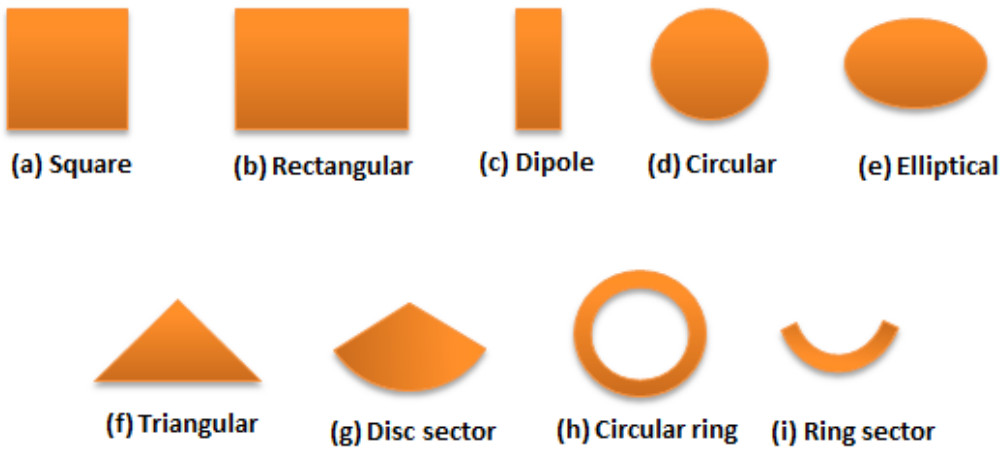

Figure 2.2 Common shapes of microstrip patch elements [15].

2.2.1. Characteristics of Microstrip Patch Antenna

The microstrip antenna has been observed to be an outstanding radiator for several applications due to its multiple benefits which can be summarised as follows:

1. Lightweight and low profile

2. Easier to integrate on printed-circuit board (PCB) with other planar circuits

3. Low cost of fabrication and therefore large scale production is possible

4. It can be customized to match the host surface

5. Facilitates dual and triple band operations

6. It can be accomplished in an extremely compact form, appropriate for personal as well as mobile communication handheld devices

7. Supports circular as well as the linear polarisation

On the flip side, there are certain drawbacks [16, 17, 18, 19 and 20]:

1. Low gain and lower power.

2. Narrow bandwidth

3. Infirm (poor) end fire radiator except for tapered slot antennas

4. External radiation of feed and intersections

5. Substandard polarisation efficacy

6. Surface wave excitation

The quality factor Q is quite high when it comes to microstrip patch antennas. Q signifies the losses pertaining to the antenna and a large Q drives low efficacy and slender bandwidth. Q can be decreased by increasing the thickness of the dielectric substrate, but this rise in thickness also increases the fraction of the total power offered by the source, which goes into a surface wave. This contribution by surface wave could be regarded as unneeded power loss as it finally gets scattered at the dielectric bends and leads to antenna characteristics degradation.

2.2.2. Applications of Microstrip Antennas

The microstrip patch antennas are renowned for their strong design, performance, fabrication and expanded use. Some of its applications are [16, 21]:

- Mobile and satellite communication
- Radio frequency identification
- Global positioning system
- Worldwide interoperability for microwave access (WiMax)
- Rectenna
- Radar
- Telemedicine
- Medicinal applications of the patch

2.2.3. Bandwidth

Antennas bandwidth is defined as a range of frequencies inside which the performance of the antenna, with esteem to some characteristic. For broadband antennas, the bandwidth is usually articulated as the ratio of the upper to lower frequencies of acceptable operation. For example, a 9:1 bandwidth shows that the upper frequency is 10 times larger than the lower. For narrowband antennas, the bandwidth is expressed is a percentage of the frequency difference (upper minus lower) over the center frequency ofthe bandwidth. For example, a 6% bandwidth shows that the frequency difference of acceptable operation is 6% of the center frequency of the bandwidth. Due to the features (polarization, input impedance, pattern, again, etc.) of the antenna does not necessarily differ in the same way or even strongly affected by frequency, there is no unique characterization of the bandwidth. The Q of antennas for arrays with dimensions large compared to the wavelength, excluding super directive designs, is near unity. iSo the bandwidth is frequently expressed in terms of beamwidth, sidelobe level, and pattern features [21]. Higher data rates, a saturation of ithe frequency spectrum, low power consumption, etc. are some of the reasons why ultra-wideband has been of increased interest over the past years. ultra-wideband(UWB), in comparison with conventional or narrow bands, using a wide bandwidth to transmit

data. The power used over the whole band is much lower than the power used by narrowband systems, ultra-wideband technology interference is produced, as the power level transmitted is almost at the noise level of the systems using the same spectrum, making it possible to share the spectrum and space with other established technologies. The federal communications commission (FCC) first defined UWB as any system having a bandwidth of at least 500 MHz. In 2002 the FCC allowed the frequency band between 3.1GHz and 10.6 GHz for unlicensed ultra-wideband transmission [22].

2.2.4 Gain

The gain of an antenna in a given direction is defined as the ratio of the intensity, in a given direction, to the irradiation intensity that would be obtained if the power accepted by the antenna were irradiated isotropically. The radiation intensity corresponding to the isotropically radiated power is equal to the power accepted (input) by the antenna divided by 4π. When the direction is not stated, the power again is usually taken in the direction of maximum radiation. in most cases, we deal with relative again, which is defined as the ratio of the power again in a given direction into the power again of a reference antenna in its referenced direction. The power input must be the same for both antennas. The reference antenna is usually a dipole, horn, or any other antenna whose again can be calculated for it is known [22].

2.2.5 Bandwidth Enhancement Techniques

In its usual shape, MSA cannot permit multi-octave bandwidth because of its resonant characteristics. Certain MSA configuration modification is needed to attain an octave bandwidth. In case a patch of rectangular shape without a ground plane and the substrate is supplied by a coaxial feed at the edge with an orthogonally shaped ground plane, then it will have an adequate dielectric constant equivalent to one with big h (that is, thickness). This adjusted configuration can be regarded as a rectangular monolithic structure. There are also circular, hexagonal, triple, and elliptical shapes monopoles configurations which give wide bandwidth [23].

A. Modified Shape Patches

The normal formations of MSA, like rectangular and circular patches, have been altered to the rectangular ring as well as a circular ring, in order to improve the bandwidth. The bandwidth should be larger since the factor of quality Q of patch resonator is decreased, which is because of the little amount of energy being stored under the patch and greater radiation. When another shape is in the patch and the cutting of U-shaped slot is carried out, this provides reinforcement to the bandwidth.

B. Planar Multi-Resonator Configurations

The resonant modulator, connected to several mRNAs, generates a broad bandwidth similar to that in multi-tuning circuits. Several of the existing configurations generate 5–25% of bandwidth. Different parasitic points, such as tapered strips, rectangular flexures, and rectangular wavy-long wavelengths, advanced the hole in the main rectangular patch. These formations generate several BWs but have these disadvantages their size is large, rendering them inappropriate as an element of the array, and there is a disparity in the pattern of the radiation over the impedance BW.

C. Multilayer Configurations

In the multilayer configurations, piled two or more than two patches on multiple layers of the dielectric substrate. On the basis of the coupling procedure, certain configurations are described as electromagnetically-coupled or aperture-coupled MASs [23].

D. Electromagnetically Coupled MSAs

In the case of electromagnetically-coupled MSA, a single patch or more at multiple layers of the dielectric substrate have coupled electromagnetically to the feeding line placed at the bottom layer of dielectric. By turns, a coaxial probe supplies power to one patch and another is coupled electromagnetically. Either the top or the bottom patch is fed using a coaxial probe. The patches are manufactured on distinct substrates, thus the dimensions of the patch are to be adjusted in order that the patches' resonant frequencies are similar to one another to generate a wide BW.

E. Stacked Multi-Resonator MSAs

The multi-resonant resonators and planar methods are integrated to raise the BW gain. One circular or rectangular patch was utilized on the layer at the bottom to induce several circular or rectangular points on the layer on the top, correspondingly. Besides BW increase, these configurations also play an important role in the profit increase [23].

2.2.6 Gain Enhancement Techniques

Major operational disadvantages of microstrip antennas are low gan and low power. However, there are methods, such as increasing the height of the substrate, that can be used to extend the efficiency (to as large as 90 percent if surface waves are not included) and bandwidth (up to about 35 percent) [24]. However, as the height increases, surface waves are introduced which usually are not desirable because they extract power from the total available for direct radiation (space waves). There are a lot of researchers using several techniques to overcome the limitation of the gain with taking into consideration the size of the antenna below we will describe most popular methods that have been used in the last decades.

A. Metamaterial

The metamaterial (MTM) can be defined as an artificial material that has unique properties not found in nature. MTMs are made from the composition of different materials (dielectric and conductor) engineered in a way to give negative constitutive parameters (μ and/or ε). The properties of MTM depend on the shape, orientation, arrangement and unit cell size. The MTM classified to the main two parts single negative metamaterial and double negative metamaterial that will be discussed detailedly at the end of this chapter.

B. Polarization-Insensitive AMC Structure

A polarization-insensitive dual-band artificial magnetic conductor (AMC) includes of a planar array of annular ring slot printed to rectangular patches. More detals about the proposed antenna and origin of the two bands are discussed by Pooja Prakash, Mahesh P. Abegaonkar and Shiban K. Koul [25].

C. Cylindrical Shell Shaped Superstrate

A novel structure to improve patch antenna gain based on the phase compensation theory is done by Masoud Shaifian Mazraeh Mollaei, Esmaeel Zang-neh, and Masoud Feshki Farahani [26]. Driving a superstrateas a flat artificial lens over normal patch antenna,phases of disseminated electric field arrows will be identical, leading to patch antenna gain enhancement.

D. Linear Superposition Of Higher Zeros

High gain and low sidelobes were attained consuming the theory of linear superposition of modes [27]. The proposed antenna had a single feed and had a simple structure, which is inexpensive and easy to design, that the high E-plane sidelobes in the radiation pattern of the TM14 mode can be repressed by adding the contribution of TM12 mode.

2.3 Methods of Analysis

2.3.1 Transmission Line Model

The simplest means for microstrip antenna research is the technique of transmission line. This model treats rectangular microstrip as part of the transmission line. The microstrip patch antenna comprises a couple of slots emitting radiation, each of which is denoted by a corresponding acceptance which is separated by space equivalent to the length [28]. This technique of transmission line has different factor effects which are explained below.

a. Fringing field

In a microstrip antenna of rectangular shape, the fringing field appears from the edges that radiate, mainly depending on dielectric constant and the ratio of length to height. The fringing fields shown in Figure 2.3 are small when the ratio L/h is << 1 which is true for most instances [17].
Where h is the substrate thickness.

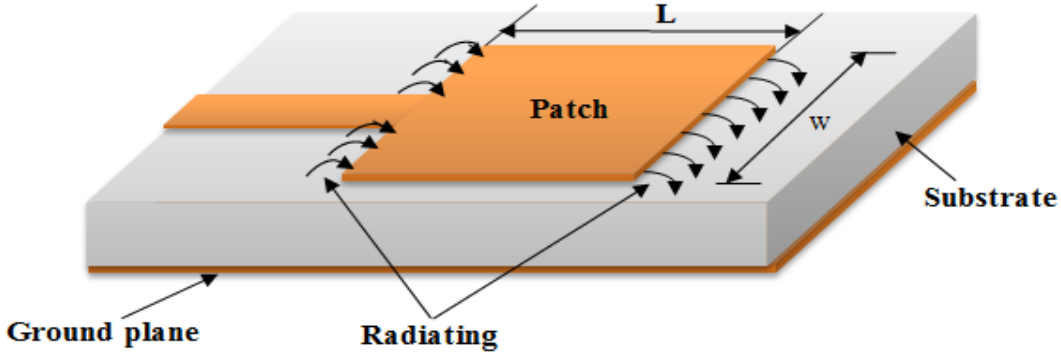

Figure 2.3 Fringing field of microstrip antenna.

When a substrate with a high dielectric constant is employed in the microstrip lines, the electric fields are nearer in the substrate. In case of substrates with lower dielectric constant, the electric fields are further which means they are far from the patch. A lower dielectric constant means more radiations and more fringing fields and it results in better performance of the antenna and higher efficiency.

The ε_{reff} for w/h>1 can be stated as [29]

$$\varepsilon_{reff} = \frac{\varepsilon_r+1}{2} + \frac{\varepsilon_r-1}{2}\frac{1}{\sqrt{1+12\frac{h}{w}}} \tag{2.2}$$

It can be observed that the lines of the fringing fields are surrounded by the substrate as well as they go far into space around as illustrated in Figure 2.4. To compute an operational dielectric constant at the time of the field lines traveling in the air and the substrate, the air should also be considered.

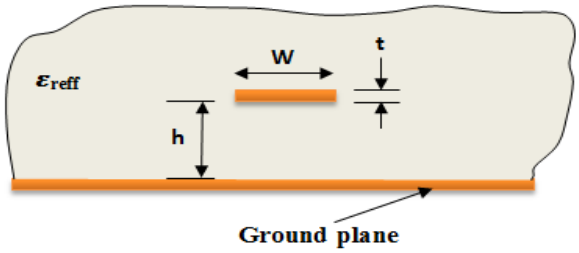

Figure 2.4 Effective dielectric constant [29]

b. Effect of fringing fields on the length

Given any rectangular patch, its actual length ΔL exceeds physical length L. As displayed in Figure 2.5, the cause is the fringing field that emerges from within the radiation slot. We, therefore, need to introduce some length extension factor in those cases where modes are established along to linear polarisations. Consideration must also be given to extending length whenever fields are generated through irradiation of the edges along its width. Normalization for the lengths and heights of insulating materials as expressed in can thus be extended.

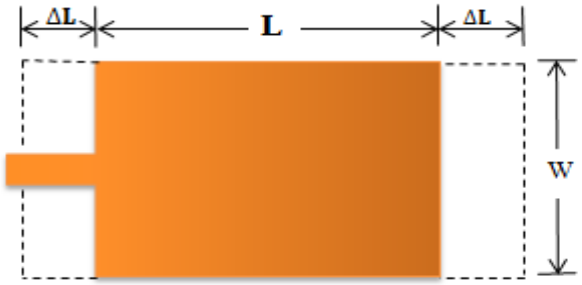

Figure 2.5 Length extension [30]

$$\frac{\Delta L}{h} = 0.412 \frac{\left[(\varepsilon_{reff}+0.3)\left(\frac{W}{h}+0.264\right)\right]}{\left[(\varepsilon_{reff}-0.258)\left(\frac{W}{h}+0.8\right)\right]} \tag{2.3}$$

Patch length represents the extension length of some 0.48 λ in place of 0.5 λ. In order to obtain the actual length for moisture that equals λ / 2, extensions for both ends must be considered, as expressed in [31].

$$L = L_{eff} - 2\Delta L \tag{2.4}$$

with dominant mode TM_{010}, patch length will equal λ/2. Thus, the L_{eff} is given by

$$L_{eff} = \frac{v_p}{f_r} \tag{2.5}$$

$$L_{eff} = \frac{C_o}{2 f_r \sqrt{\varepsilon_{reff}}} \tag{2.6}$$

where

c_o is the velocity of light in free space.

f_r is the resonance frequency.

L_{eff} is the effective length of Patch.

ν_p is the phase velocity.

c. Patch Width

With dominant mode TM_{010}, there is no reason to consider effective dielectric constant aspects, since no fringing fields are present along its width. The formula that computes the patch width is [32],

$$W = \frac{c_o}{2f_r\sqrt{\frac{\varepsilon_r+1}{2}}} \tag{2.7}$$

d. Resonance Frequency

With dominant mode TM_{010}, antennae resonate (with no consideration for fringing effect) at certain frequencies, as expressed in:

$$f_r = \frac{C_o}{2L\sqrt{\varepsilon_r}} \tag{2.8}$$

where f_r is resonant frequency

e. Input Impedance

In all cases, impedances must be matched in order to locate all points adjacent to patch spots, wherein the input resistances equal that for the corresponding feeding lines, as shown by each feeding or driving point. This input impedance for each feed point is termed the driving-point impedance. Voltages reach their maximum at corners, whereas currents reach their maximum at the centre. Naturally, resistance is calculated as the ratio of voltage to current. Resistances, therefore, reach their maximum at the corners, whereas these reach their minimum at the centre.

2.3.2 Cavity model

With microstrip antennae, whenever the regions between microstrip patches and ground plane are assumed to be resonance cavities, such approaches are collectively referred to as the cavity model [33]. This scheme is bordered with the ceiling and floor of the magnetic walls and electrical conductors positioned along the connector's edge, as displayed in Figure 2.6.

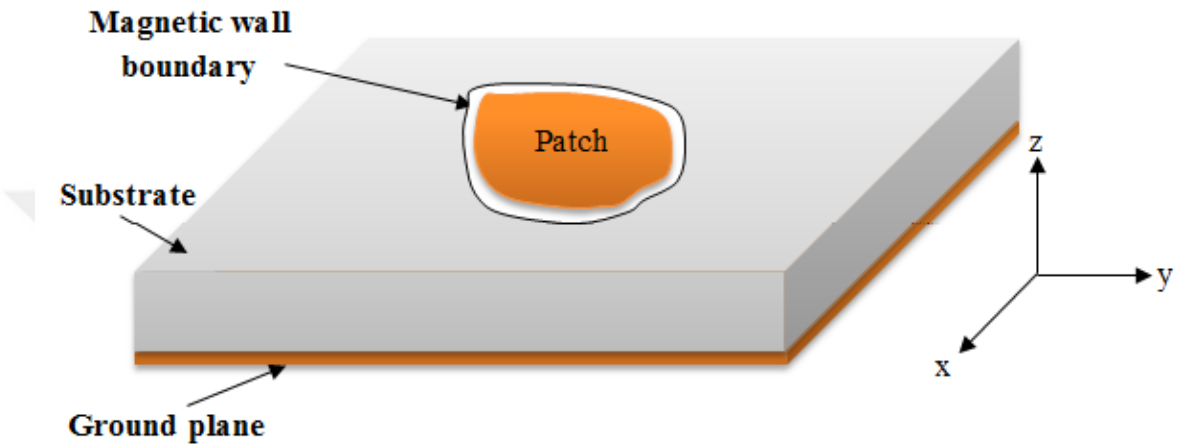

Figure 2.6 Magnetic wall model of a microstrip patch antenna [33].

The above presumption is based on:

1. Regions enclosed within this cavity generally feature only 3 field components the E component along the direction of the z-axis (E_z), plus the 2 H components along the direction of the x- as well as y-axis (H_x, H_y).

2. Fields within interior regions generally will not vary with the z-coordinates for every frequency, for *h* is extremely thin ($h<<\lambda$).

3. Electric currents in microstrip patches generally have no components that are normal to the edges of their patches at all points.

This scheme is good for examining microstrip resonances by slightly extending the edges for the purpose of calculating the emerging fringing areas. Before proceeding with calculations for the fields within a cavity, we examine its cavity mechanisms [18]. Consider the microstrip antenna depicted in Figure 2.16.

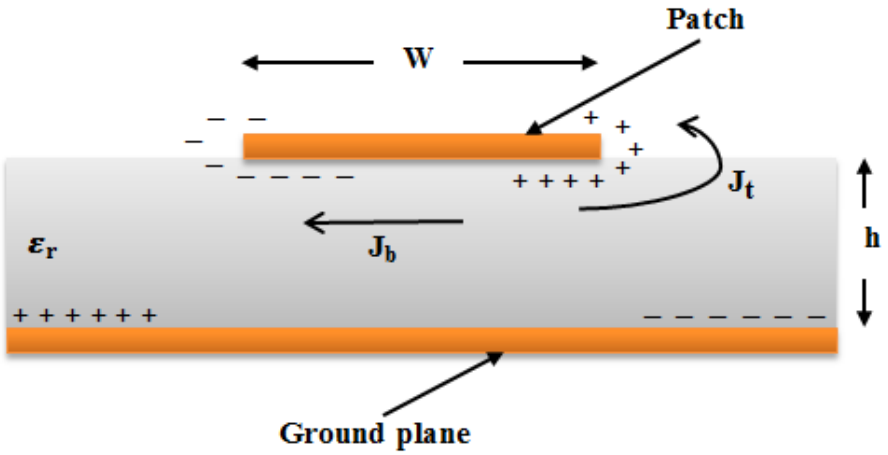

Figure 2.7 Charge distribution and a current density of a microstrip antenna [29]

When a microwave source and a microstrip antenna are connected, the establishment of the charge will take place in such a way that the distribution in the antenna's lower and the upper planes will occur in a manner similar to what is given in Figure 2.16. There are two mechanisms that control the distribution of charges attractive and repulsive. The attractive force exists between opposing charges on the earth's surface and the patch, generating the density of current J_b that can then be found at the bottom of the patch within the insulator. There is a tendency for the repelling force to push the charges originating from the bottom of the patch along the edge of the patch and all the way to the top of the patch, producing the current density J depicted in Figure 2.16.

The dominant force is the attractive mechanism when microstrip antennas are observed to exhibit w>>h and the charge concentration inside the electrical insulation happens to be below the patch. One can also disregard the current flow around the edge when it experiences a decrease with the low-to-width ratio. This makes it possible to model the four side as ideal magnetic conductive surfaces which would not cause any disturbance to the magnetic field and lead to shifts in the electric field distribution along the bottom of the patch." As a result of this good approximation for the cavity model, it is possible to deal with side walls as ideal magnetic walls.

2.4 Numerical Techniques

Several numerical techniques can be used for solving magnetic and electric fields given an arbitrarily shaped antenna geometry. These techniques can be categorized into two key groups:

2.4.1 Frequency Domain Techniques

From these techniques, the microstrip antenna was analyzed using the method of moments (MoM) and finite element method (FEM). When the method of moments is used, the antenna needs to be discretized into small segments. The currents going through the segments are a result of the known incident field and can be represented through unknown coefficients. Therefore, one can solve these coefficients by using standing numerical techniques. Once the determination of the currents is done, one can then calculate the microstrip antenna input impedance. Through the introduction of equivalent currents, MoM can be utilized with a microstrip antenna. To obtain accurate solutions, this method needs fine segments [33]. Thus, it is not an advisable solution in the microstrip antenna case.

For the FEM, discretization of the ground plane, the microstrip antenna, and the entire volume surrounding the microstrip antenna takes place and they are turned to small tetrahedrons. This process increases the problem's computational size, and yet the FEM still has numerous advantages over the MoM. For instance, FEM does not need to formulate equivalent currents and is therefore applicable to arbitrary geometries [36]. Several commercial software suites such as HFSS are established on FEM.

2.4.2 Time Domain Techniques

The analysis of time domain, two theory can be used for analyzing the microstrip antenna the transmission line matrix (TLM) theory and the finite-difference-time-domain (FDTD) method [34]. For these techniques, there is discretization of the entire volume around the microstrip antenna. Instead of using tetrahedrons, small cubes are utilized. When the curved geometries are discretized, stair stepping effect must be considered for proper modeling. When using time domain methods, the microstrip antenna is made to undergo excitation using a wideband pulse. The solution is then turned into the frequency domain, which determines the input impedance given a broad frequency range. For frequency domain methods, there is a repetition of the input impedance calculations for every frequency to determine the input impedance given the frequency range. However, this process is time-consuming. Finite Integration

Technique (FIT) is considered a general form of the FDTD method. Instead of using the differential forms of Maxwell's equations, it uses the integral ones [34].

2.5 CST Microwave Studio

Computer simulation technology (CST) microwave studio serves as a simulation tool for verifying the accuracy of the numerical results. The basis for the CST is the FIT with the perfect boundary approximation (PBA). The FIT has links with the FEM and is also popularization of the finite difference time domain [33].

For this method, discretization of the integral form of Maxwell's equations is done instead of the differential form. The PBA mesh possesses excellent convergence properties. A huge memory is not needed to conduct the simulation. Alternatively, it is appropriate to use the PBA mesh to simulate the large structures since it can quickly obtain the simulated results. In a comparison between the tetrahedral mesh and the PBA staircase mesh, the PBA mesh is considered the best based on the low memory requirements [33].

Furthermore, the tetrahedral mesh possesses perfect assemblage properties. However, if large structures need to be simulated, large memory and longer simulating times are required. In cases of staircase mesh utilization, simple structures that do not have curved structures are more appropriate since curved structures will fail to converge within a reasonable computing time [34]. CST microwave studio is only utilized for the verification of the first step antenna design and for ensuring that the produced antennas will be working as efficiently as possible. In this study, the CST microwave studio was utilized for the simulation of the characteristics of the antennas being proposed.

2.6 Metamaterial

The metamaterial (MTM) can be defined as an artificial material that has unique properties not found in nature. MTMs are made from the composition of different materials (dielectric and conductor) engineered in a way to give negative constitutive parameters (μ and/or ε) [35, 36, 37]. The properties of MTM depend on the shape,

orientation, arrangement and unit cell size. Figure 2.8 shows some MTM shapes. The unit cell MTM size, p, needs to be smaller than the wavelength to avoid the electromagnetic wave diffraction as shown in Figure 2.9.

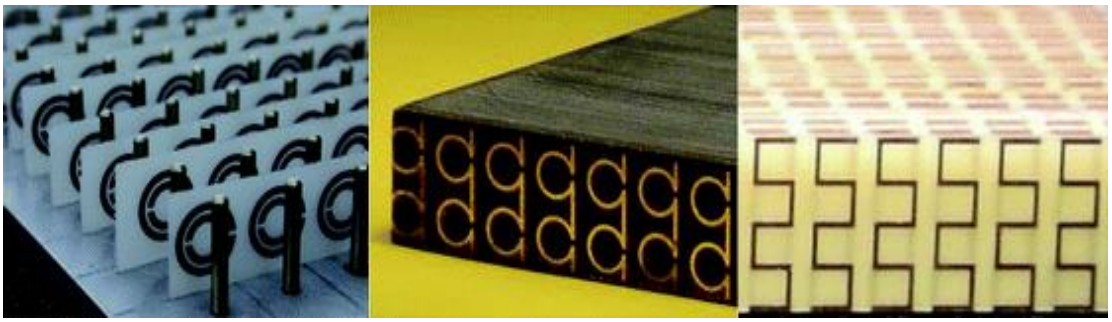

Figure 2.8 Some MTM shapes.

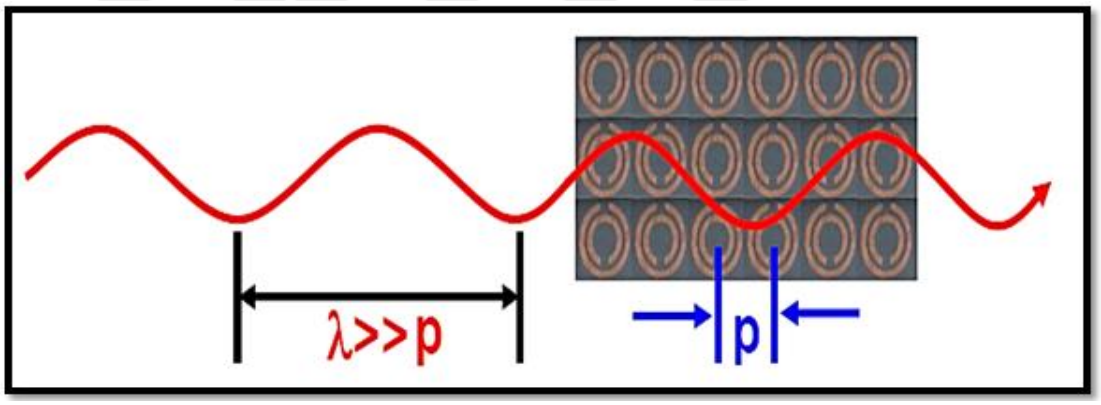

Figure 2.9 Unit cell size compared with the wavelength.

2.6.1 History of Metamaterial

MTM concern known at the end of the 19th century. The first MTM introduced by Jagadish Chandra Bose in 1898 as a chiral structure.

In the 20th century, Karl Ferdinand Lindman studied the wave interaction with metallic helices as artificial chiral media. In the 1940s, Winston E. Kock developed materials that have the same characteristics of the metamaterial. In the duration between the 1950s and 1960s, the artificial dielectrics studied for lightweight microwave antennas.

In 1967, the Russian physicist Viktor Veselago achieved substances with negative permittivity and permeability. Veselago showed these materials can achieve a phase velocity anti-parallel to the Poynting vector direction where this is opposed to the wave propagation in natural materials [38].

Microwave radar absorbers were started as applications for artificial chiral media in the 1980s and 1990s [36].

Later, John Pendry introduced the first practical way to achieve MTM properties not subject to the right-hand rules. The idea is presented by putting a wire along the wave direction. The result showed a negative permittivity ($\varepsilon < 0$) [39]. Negative permittivity wasn't the challenge because there are some of the natural materials show the negative permittivity. The Pendry's challenge was in achieving a material shows a negative permeability ($\mu < 0$).

Later, Smith et al. repeated the Pendry experiments by using wires and split ring together in one structure then placed it along the wave propagation direction. The result showed a negative ε & μ [41, 42, 43].

2.6.2 Classification of Electromagnetic Metamaterials

MTMs are classified according to the properties, characteristics, and the value of the constitutive parameter. The electromagnetic MTM divided into two main types of single negative MTM (SNG), and double negative MTM (DNG). Each one of these types is characterized by different properties that distinguish it from other material.

A. Single Negative Metamaterial

The Single Negative Metamaterial, SNG, is the second type of the MTM characterized by a negative ε or negative μ but not both.

The first type of SNG is with $-\varepsilon$, epsilon negative (ENG), MTM that characterized by $-\varepsilon$ with positive μ as shown in Figure 2.10 [35, 44]. The refractive index formula of the ENG MTM is given as:

$$n = \sqrt{(-\varepsilon_r)(+\mu_r)} = j\sqrt{\varepsilon_r\,\mu_r} \tag{2.9}$$

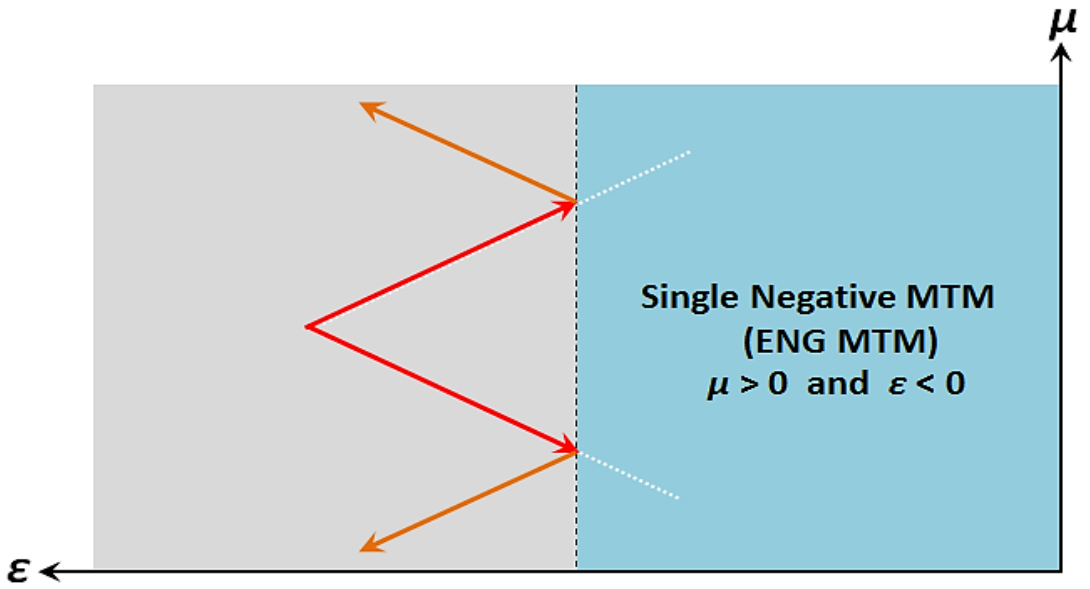

Figure 2.10 Electromagnetic wave behavior in the ENG MTM medium.

The second type of SNG is with mue negative -μ, MNG, MTM that characterized by -μ with positive ε as shown in Figure 2.11 [35, 44]. The refraction index formula of MNG MTM is given as:

$$n = \sqrt{(+\varepsilon_r)(-\mu_r)} = j\sqrt{\varepsilon_r\,\mu_r} \tag{2.10}$$

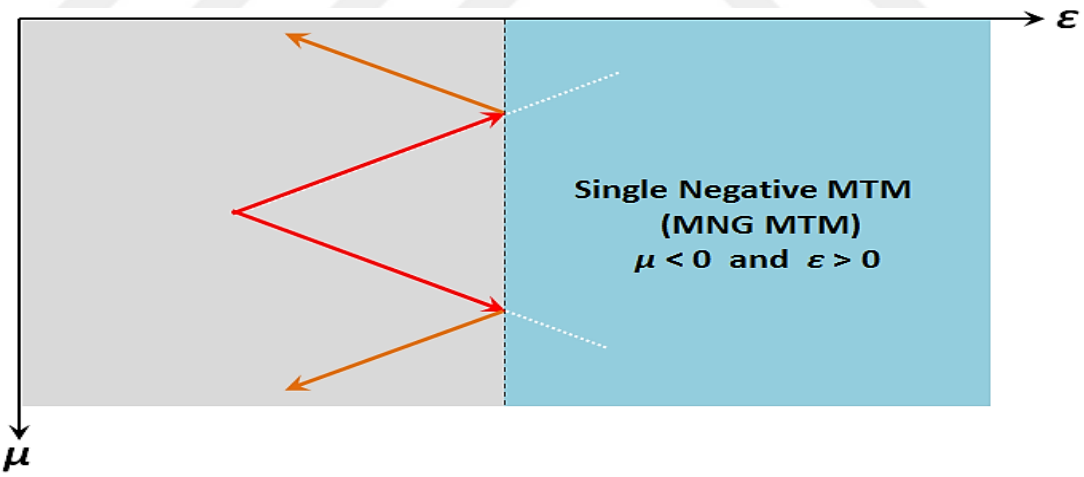

Figure 2.11 Electromagnetic wave behavior in the MNG MTM medium

Finally, the SNG in both types, ENG and MNG, are characterized by an imaginary refractive index which no wave passes through it and all the incident waves will be reflected [35, 44].

B. Double Negative Metamaterial

The double negative metamaterial, DNG MTM, or known by left hand MTM [35], is one of MTMs type that characterized by $-\varepsilon$ and $-\mu$. The property of such material is unique and not found in nature [44]. The effect of $-\mu$ and $-\varepsilon$ is presented by refracting the wave with a negative sign and direct it to another direction instead of the forward direction as shown in Figure 2.11. The refraction index formula is given as [44].

$$n = \sqrt{(-\varepsilon_r)(-\mu_r)} \tag{2.11a}$$

$$n = \sqrt{-1} \times \sqrt{-1} \times \sqrt{\varepsilon_r \mu_r} \tag{2.11b}$$

$$n = j \times j \times \sqrt{\varepsilon_r \mu_r} = j^2 \times \sqrt{\varepsilon_r \mu_r} \tag{2.11c}$$

$$n = -\sqrt{\varepsilon_r \mu_r} \tag{2.11d}$$

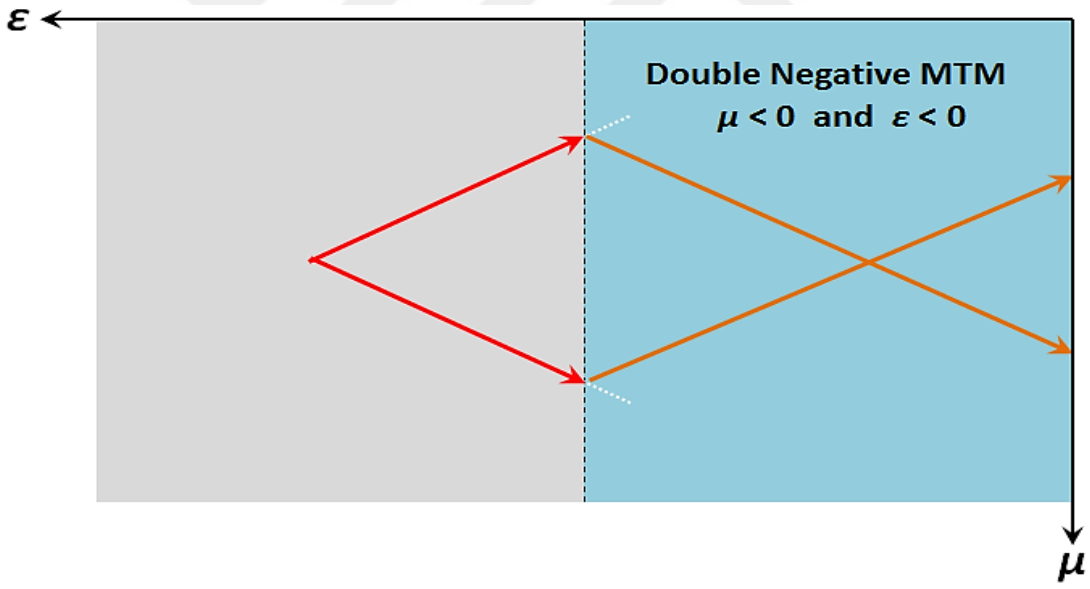

Figure 2.11 Electromagnetic wave behavior in the DNG medium

2.6.3 Metamaterial Applications

Due to the MTM unique properties, a significant change in the antenna surface wave, quality factor, current distribution, and antenna radiation pattern may be achieved [45].

In the gain and directivity improvement, the MTM is divided into two parts the first part is presented DNG and SNG, where such materials can be used to focus the antenna radiation by decreasing the beamwidth of the antenna main lobe and achieve more power intensity in narrow beam in order to enhance the antenna gain and directivity. While the other type of MTM is presented by SNG used to enhance the gain and directivity of the antenna that suffers from back and side lobs by reflecting and re-directing these lobes to the main lobe direction. Moreover, all the previous MTM types can reduce the antenna surface waves that lead to enhancing the antenna gain.

In the antenna bandwidth enhancement, the MTM can be used in the antennas that suffer from narrow bandwidth to improve their performance by reducing the antenna quality factor. Moreover, increase the antenna matching leading to minimum wave reflecting.

CHAPTER 3

A PARTIAL GROUND PLANE MICROSTRIP PATCH ANTENNA FOR WIDEBAND APPLICATION

3.1 Introduction

It is still a challenge to find a competitive antenna for the enforcement of UWB systems. Planar antennas are considered the best choice for UWB radio system because of low cost, lightweight and low profile. Mainly, the printed antenna has a very important part as follows the patch and the ground-level radiator is the etched opposite site the substrate of PCBs. In some configurations, the ground plane may be coplanar with a patch. The patch can be fed by microstrip line and coaxial cable.

In this chapter, a UWB partial ground plane printed patch antennas is proposed to be used in UWB applications. The proposed antenna is a double transition step printed patch antenna, which consists of a rectangular patch with two rectangular transition steps and has a partial ground plane printed on the obverse sides of the substrate. The radiator of such antenna, rectangular patch based double transition steps, is fed through a 50 Ω microstrip line.

The computer simulation technology (CST) software package is used to design and simulate the antenna structures.

3.2 Antenna Design Methodology

The design steps of the microstrip patch antenna structure starting from the conventional profile until arriving at the optimum structure is discussed in this section. The antenna design methodology can be summarized in three main steps as follows:

- Design the conventional microstrip patch Antenna profile.
- Applying the transition steps on the conventional microstrip patch antenna profile.
- Applying the partial ground plane technique on the microstrip patch antenna.

3.3 Conventional Microstrip Patch Antenna

3.3.1 Antenna Design.

The conventional microstrip patch antenna design that is shown in Figure 3.1 consists of four main structures a substrate, a rectangular patch, a ground plane, and a feed line. The substrate is picked as FR4-Epoxy with dielectric constant and loss tanδ equals to 4.4 and 0.02, respectively. The substrate dimensions are 38×36 mm^2 with a thickness of 1.58 mm, which is small enough to embed inside the circuit boards for many wireless communication applications.

The second part of the antenna construction is the rectangular patch that mounted on the dielectric substrate, which is made of copper metal with dimensions equals to 18 ×20 mm^2 and thickness of 17mm.

The ground plane is the third part of the antenna construction that made of copper metal with dimensions of 38×36 mm^2 printed on the substrate bottom.
The feed line is the last part of the antenna construction. The direct coupling feeding technique presented by the microstrip line is used to feed the proposed antenna. The microstrip line of the proposed antenna is etched on the top of the substrate connecting between the rectangular patch and the source. The microstrip line is picked as a copper metal with dimensions of choice to gives 50 Ω. Finally, the other related dimensions details of the proposed antenna are presented in table 3.1.

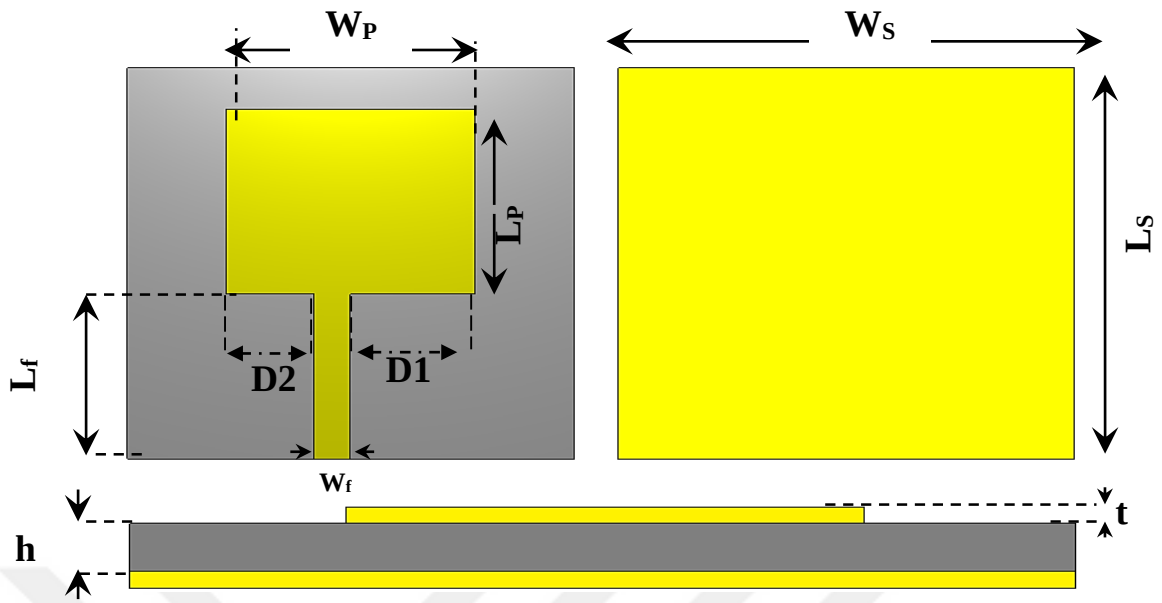

Figure 3.1 Conventional microstrip patch antenna (a) top view, (b) back view, (c) side view.

Table 3.1 Conventional Microstrip Patch Antenna.

Parameter	Dimensions(mm)
L_S	38
W_S	36
L_P	18
W_P	20
L_f	16
W_f	2.13
h	1.58
t	17
D1	10
D2	7

3.3.2 Simulation Results

In this section, the antenna performance is discussed in terms of S_{11}, the voltage standing wave ratio (VSWR) and the gain.

A. Antenna S_{11} and VSWR

The performance of the proposed design model based conventional microstrip patch antenna structure is tested numerically in terms of S_{11} as seen in Figure 3.2. It is found that the proposed antenna model provides an S_{11} < -10 dB at the frequency bands 7.445 GHz - 8.1146 GHz, 10.403 GHz - 10.775 GHz, 11.069 GHz - 11.923 GHz, and from 12.1341 GHz, 14.2 to 20 GHz. The antenna behaves like a multiband antenna.

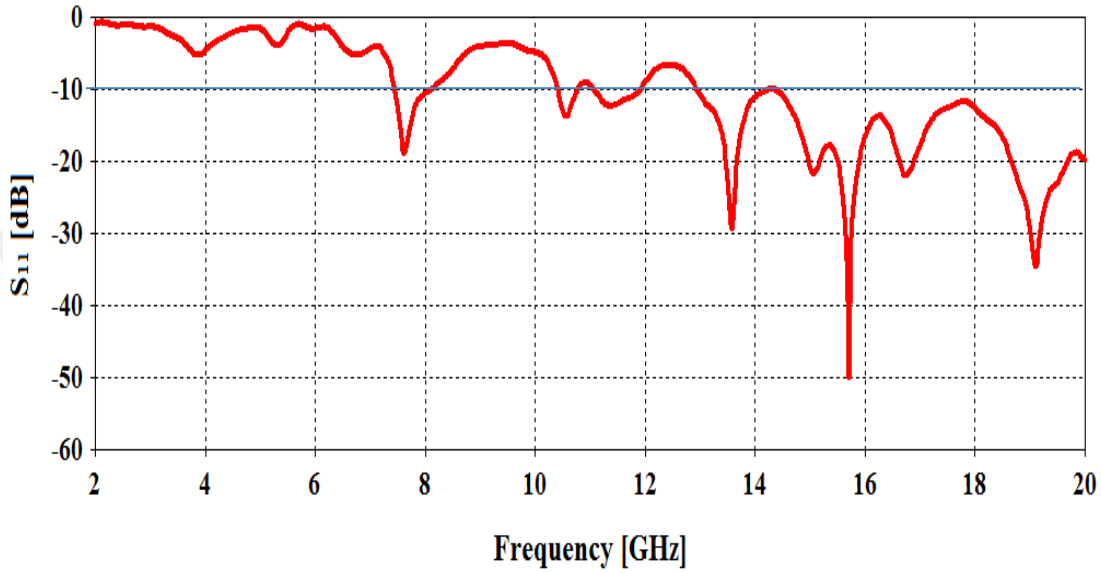

Figure 3.2 S_{11} of the conventional microstrip patch antenna.

In addition to the S_{11}, the VSWR is found as seen in Figure 3.3. It's found that, the antenna shown VSWR less than 2 at the frequency bands 7.445 GHz - 8.1146 GHz, 10.403 GHz - 10.775 GHz, 11.069 GHz - 11.923 GHz, and from 12.1341 GHz to 20 GHz.

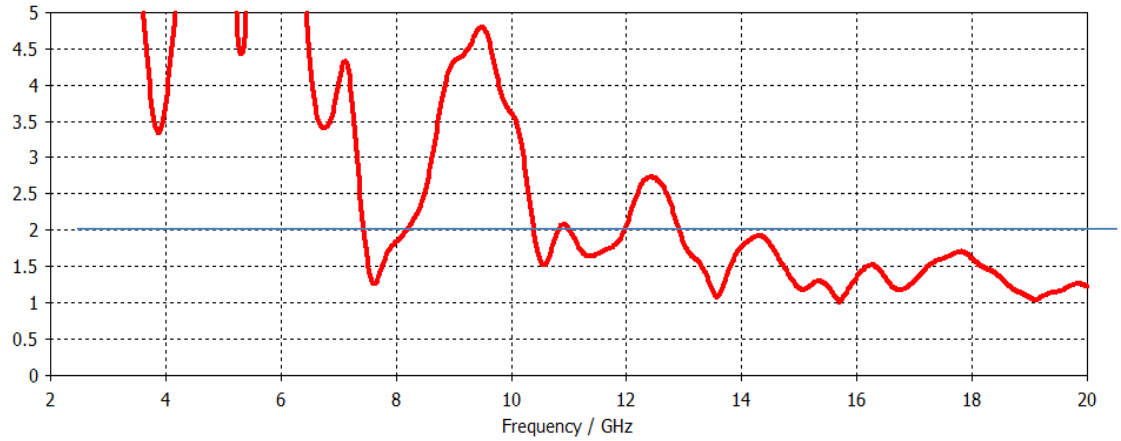

Figure 3.3 VSWR of the conventional microstrip patch antenna.

B. Antenna Gain and Directivity

The gain is the amount of the radiated energy of the ann antenna and the gain of the proposed antenna are evaluated as a function of frequency as seen in Figure 3.4. It's found that the gain value of the proposed antenna is varying from 2 dB to 5.424 dB at different frequency modes as seen in table 3.2.

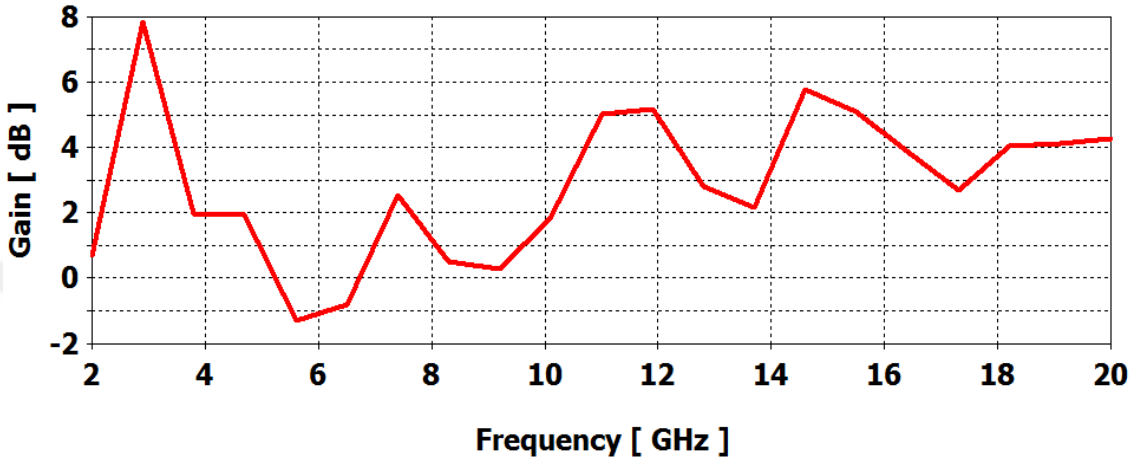

Figure 3.4 Gain of the conventional microstrip patch antenna.

In addition to the antenna gain, the directivity is the capability of the antenna to send and receive the signal over the directivity of the proposed antenna is evaluated as a function of frequency as seen in Figure 3.5. It's found that the directivity value of the proposed antenna is varying from 6.1067 dB to 10.166 dB at different operating frequency modes as seen in Table 3.2.

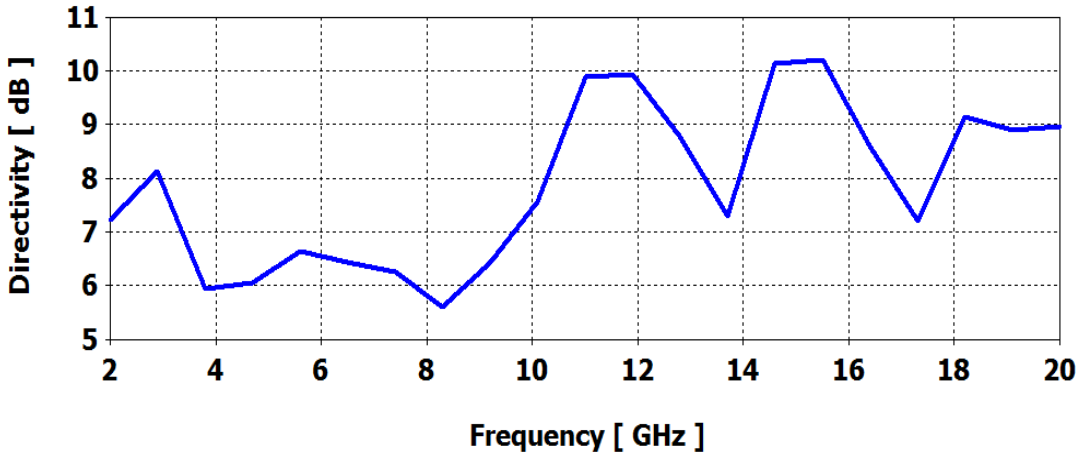

Figure 3.5 Directivity of the conventional microstrip patch antenna.

Table 3.2 Gain and Directivity Values of The Conventional Microstrip Patch Antenna at Different Operating Modes.

Frequency (GHz)	Gain (dB)	Directivity (dB)
7.616	2.0659	6.1067
10.558	3.4534	8.7487
11.4	5.0872	9.9104
13.571	2.2444	7.4985
15.067	5.424	10.166
15.698	4.8426	9.8503
16.742	3.43	8.0661
19.1	4.1215	8.8924

3.4 Transition steps Microstrip Patch Antenna

Transitions steps are applied to the bottom of the microstrip patch antenna that is achieved in the previous section as an attempt to increase antenna performance by decreasing the energy that sorted in the substrate in order to increased bandwidth before adding the partial ground plane.

3.4.1 Antenna Design

In Figure 3.6, the microstrip patch antenna based on transition steps is presented. The proposed antenna construction is contained in four main parts which are patch, ground, substrate, and transmission line, as in the previous antenna, conventional microstrip patch antenna.

The proposed antenna, microstrip patch antenna based on transition steps, is characterized by having the same dimensions of the previous antenna, which is 38×36 mm^2 with substrate thickness equals to 1.58 mm. The other related dimensions of the proposed antenna can be found in Table 3.3.

The main difference between such an antenna and the previous one is presented in the transition steps that are located between the microstrip transmission line and rectangular radiating patch as seen in Figure 3.9 (a).

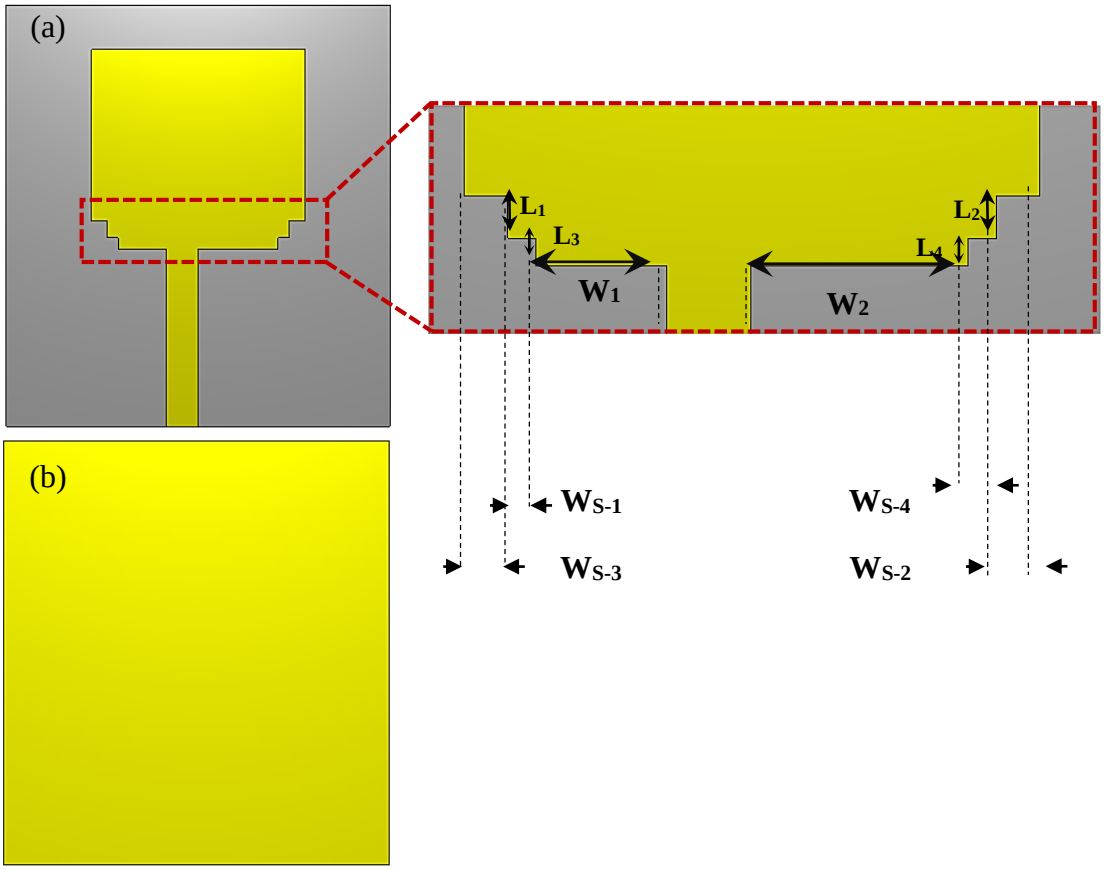

Figure 3.6 Microstrip patch antenna based on transition steps, (a) top view, (b) bottom view.

Table 3.3 Microstrip Patch Antenna with Transition Steps.

Parameter	Dimensions(mm)
L_1	1.5
L_2	1.5
L_3	1
L_4	1
W_1	4.55
W_2	7.55
W_{S-1}	1
W_{S-2}	1
W_{S-3}	1.5
W_{S-4}	1.5

3.4.2 Simulation Results

In this section, the antenna performance is discussed in terms of S_{11}, the voltage standing wave ratio (VSWR), gain, directivity, current distribution, and radiation patterns.

A. Antenna S_{11} and VSWR

The performance of the proposed design model based on a transition steps structure is tested numerically in terms of S_{11} as seen in Figure 3.7. It is found that the proposed antenna model provides an S_{11} < -10 dB at the frequency bands 7.7101 GHz - 8.6743 GHz, 10.8578 GHz - 11.5432 GHz, and from 13.25319 GHz to 20 GHz.

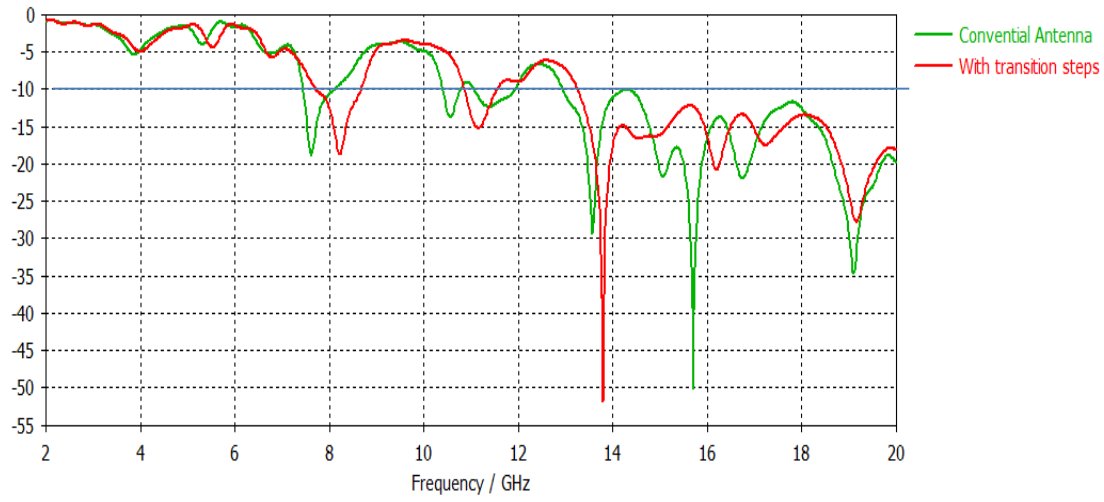

Figure 3.7 S_{11} of the microstrip patch antenna with transition steps and S_{11} of the conventional antenna.

In addition to the S_{11}, the VSWR of the proposed antenna is found as seen in Figure 3.8. It's found that, the antenna shown VSWR less than 2 at the frequency bands 7.7101 GHz - 8.6743 GHz, 10.8578 GHz - 11.5432 GHz, and from 13.25319 GHz to 20 GHz.

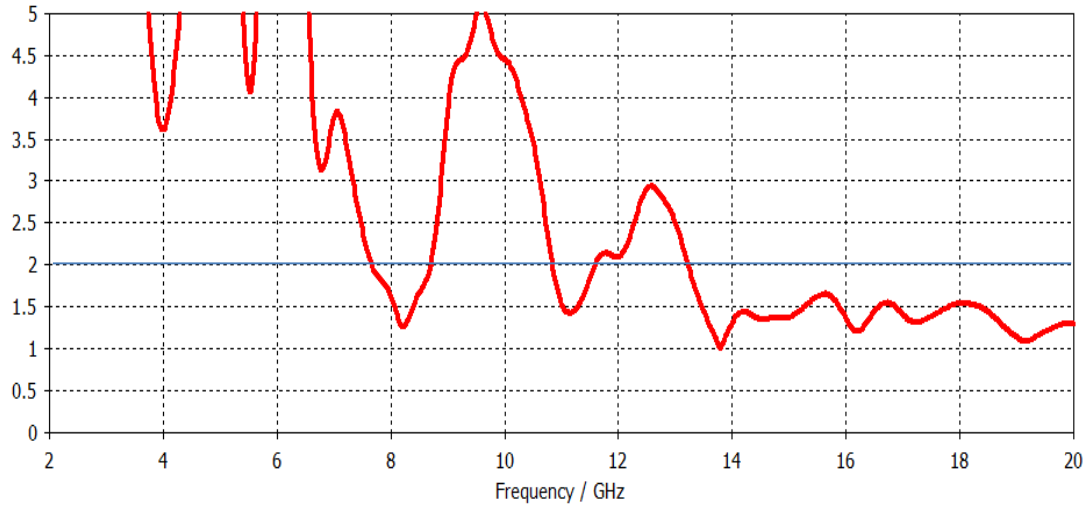

Figure 3.8 VSWR of the transition steps microstrip patch antenna.

B. Antenna Gain and Directivity

After applying the transition steps the gain of the proposed antenna is evaluated as a function of frequency as seen in Figure 3.9. It's found that the gain value of the proposed antenna is varying from 1.1247 dB to 4.2328 dB at different frequency modes as seen in table 3.4.

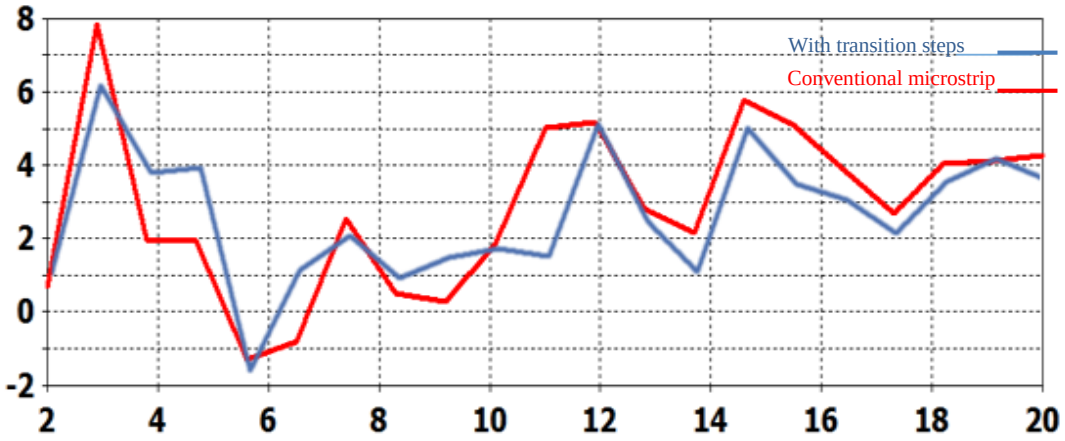

Figure 3.9 Gain of the microstrip patch antenna with transition steps.

In addition to the antenna gain, the directivity of the proposed antenna is evaluated as a function of frequency as seen in Figure 3.10. It's found that the directivity value of the proposed antenna is varying from 5.8106 dB to 9.0587 dB at different operating frequency modes as seen in table 3.4.

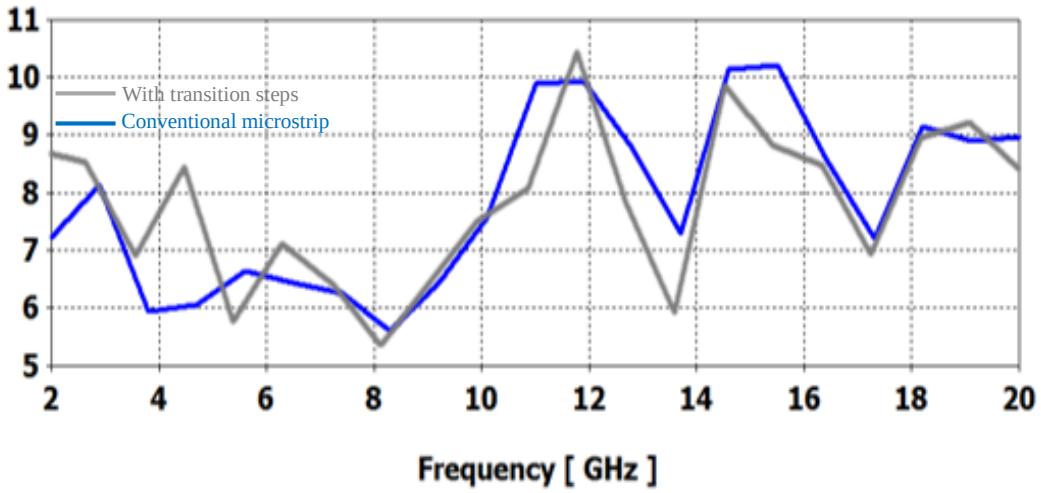

Figure 3.10 Directivity of the microstrip patch antenna with transition steps

Table 3.4 Gain and Directivity Values of The Microstrip Patch Antenna with Transition Steps at Different Operating Modes.

Frequency (GHz)	Gain (dB)	Directivity (dB)
8.2212	1.1247	5.8106
11.147	2.1848	8.4513
13.79	1.5927	6.5548
16.202	3.2428	8.521
17.229	2.3129	7.2158
19.154	4.2328	9.0587

3.5 A Partial Ground Plane Microstrip Patch Antenna

A partial ground plane technique is applied to the microstrip patch antenna with the transition Steps that is designed in the previous section. This technique is used as an attempt to improve the antenna performance such as bandwidth by reducing the energy stored in the substrates and increased the matching between the transmission line impedance with the input impedance to make sure the energy transmitted from the source to the patch perfectly.

3.5.1 Antenna Design

In Figure 3.11, a partial ground plane of the microstrip patch antenna is presented. The proposed antenna structure has the same constructing parts patch, substrate, and

transmission line, but with the partial ground plane instead of the full ground plane as in the previous antennas, conventional microstrip patch antenna with transition steps.

The proposed antenna has the same patch shape and size of the microstrip antenna with transition partial ground plane, the other related dimensions of the proposed antenna can be found in Table 3.5.

The main difference between such an antenna and the previous one is presented by the partial ground plane with a slot as seen in Figure 3.17. This technique works to improve the antenna bandwidth. Basically, the action of the decreasing energy located in the substrates by partial grounds this decreasing of the stored energy in the substrates leads to reduce in the quality factor of the antenna and the bandwidth will be increased. Partial ground plane means back radiation. Therefore, more radiation loss. Hence, the Q factor decreases and as a result of that, bandwidth increases.

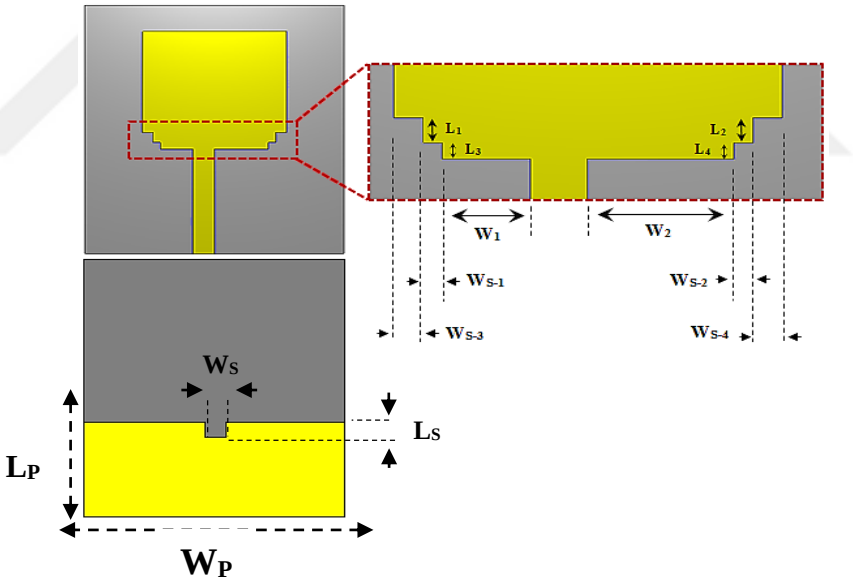

Figure 3.11 Microstrip patch antenna with a partial ground plane.

Table 3.5 Microstrip Patch Antenna with Partial Ground Plane.

Parameter	Dimensions(mm)
L_1	1.5
L_2	1.5
L_3	1
L_4	1
W_1	4.55
W_2	7.55
W_{S-1}	1
W_{S-2}	1
W_{S-3}	1.5
W_{S-4}	1.5
L_P	15
W_P	36
L_S	2.7
W_S	3.8

3.5.2 Simulation Results

In this section, the antenna performance is discussed in terms of S_{11}, the voltage standing wave ratio (VSWR), gain, directivity.

A. Antenna S_{11} and VSWR

The performance of the partial ground plane microstrip patch antenna structure is tested numerically in terms of S_{11} as seen in Figure 3.12. It is found that the proposed antenna model provides a frequency band from 2.616 GHz to more than 20 GHz. By this way, we obtain a UWB antenna.

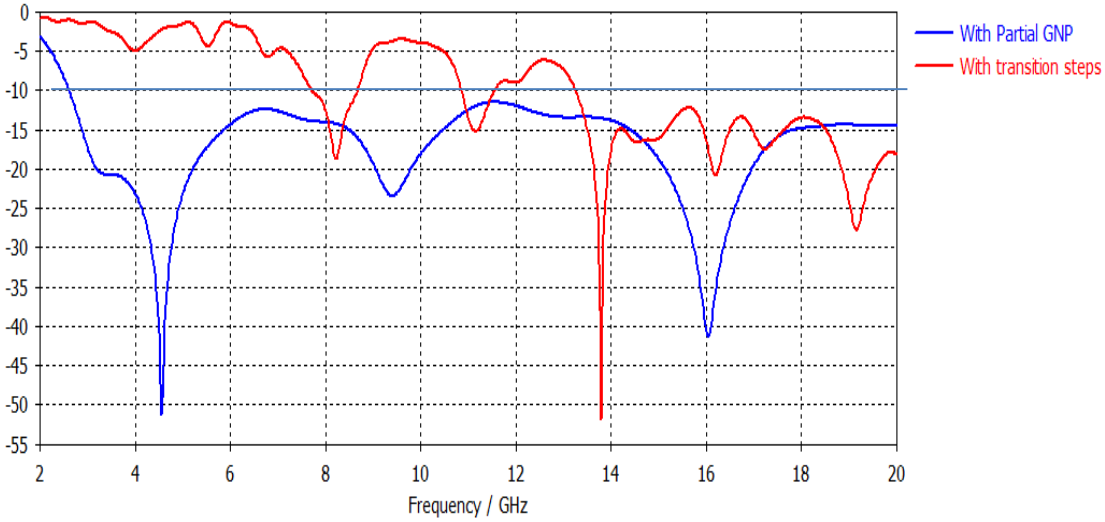

Figure 3.12 S_{11} of the microstrip patch antenna with partial ground plane and microstrip patch antenna with transition steps

In addition to the S_{11}, the VSWR of the proposed antenna is found as seen in Figure 3.13. It's found that the antenna provides VSWR less than 2 at the frequency bands starting from 2.616 GHz and continuous to more than 20 GHz.

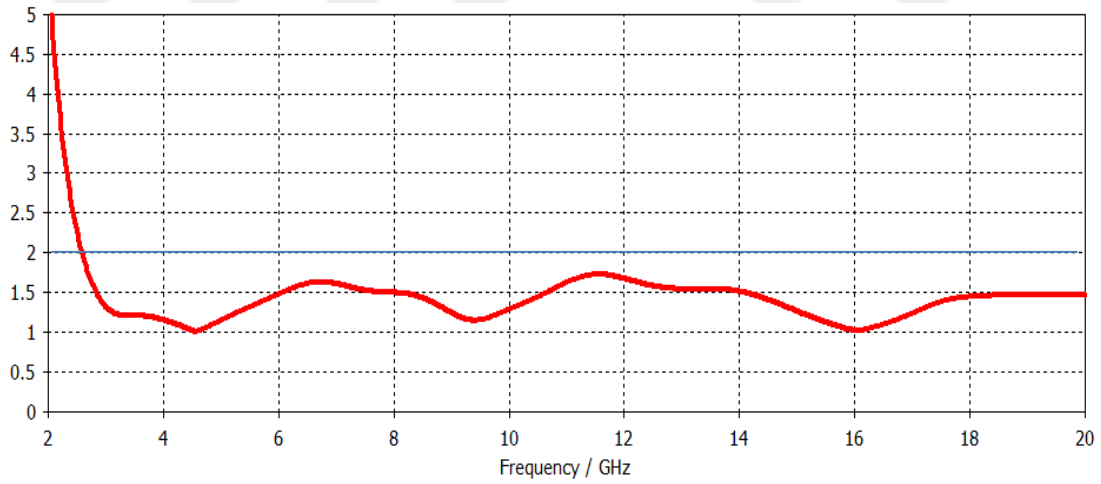

Figure 3.13 VSWR of the microstrip patch antenna with a partial ground plane.

B. Antenna Gain and Directivity

The gain of the proposed antenna is evaluated as a function of frequency as seen in Figure 3.14. It's found that the gain value of the proposed antenna is varying from 1.24 dB to 5.6 dB at the different operating frequency.

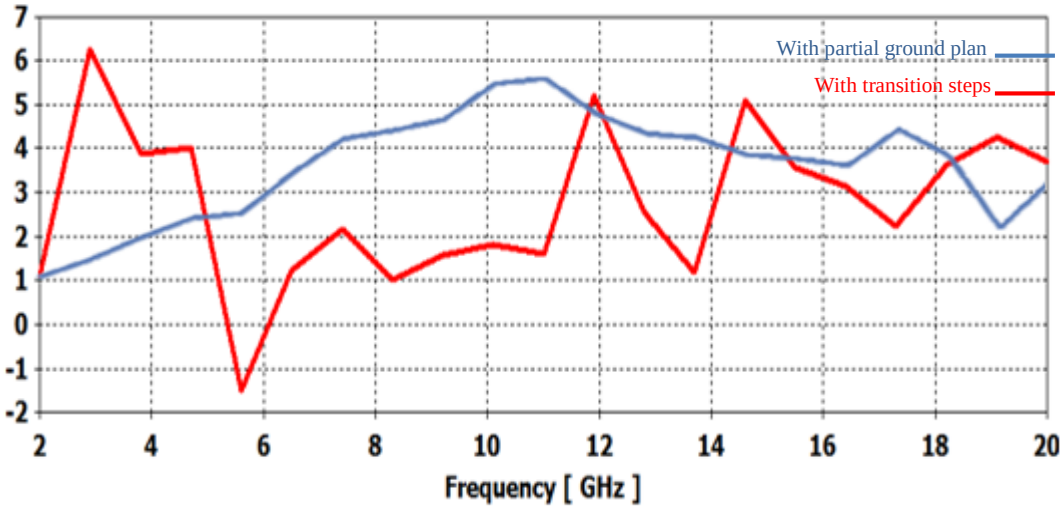

Figure 3.14 Gain of the of the microstrip patch antenna with a partial ground plane.

The directivity of the proposed antenna is evaluated as a function of frequency as seen in Figure 3.21. It's found that the directivity value of the proposed antenna is varying from 2.26 dB to 7.1 dB at the different operating frequencies.

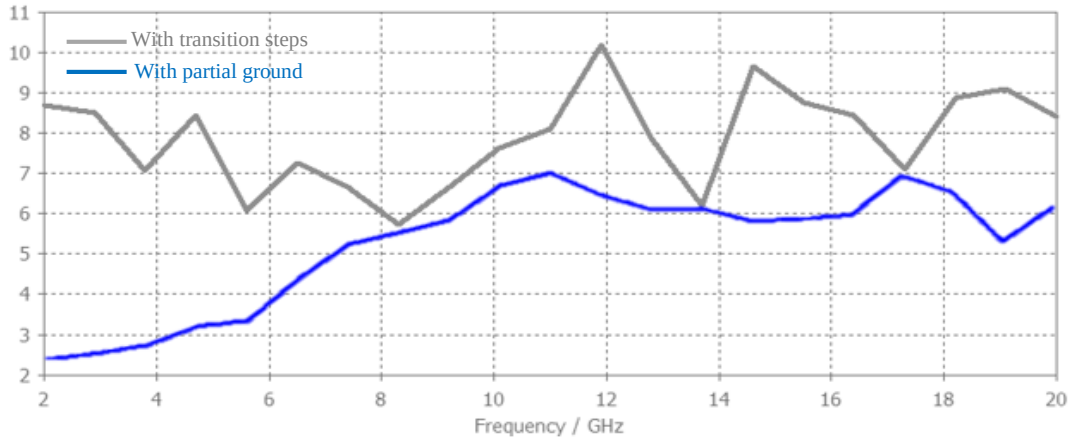

Figure 3.15 Directivity of the microstrip patch antenna with a partial ground plane.

CHAPTER 4

UWB MICROSTRIP PATCH ANTENNA WITH TSRR METAMATERIAL STRUCTURES

4.1. Introduction

After designing the conventional microstrip patch antenna and improved the antenna matching and bandwidth by applying two techniques, transition steps and partial ground plane techniques, the next step is presented by enhancing the antenna gain and directivity of the proposed antenna by using the metamaterial structures

The objective of this chapter is to discuss and design UWB microstrip antenna based on metamaterial structures. In section 4.2 the proposed structure is consisting of a 2×1 array of MTM unit cells located above the antenna. The main purpose of the addition the MTM to the antenna is to enhance the antenna gain and directivity.

The optimal design and the effects of adding MTM structures on antenna performance are identified based on numerical simulations. In order to investigate the performance of the MTM and antenna designs, they are conducted with a FIT based on CST MWS formulation.

4.2 Literature Survey

4.2.1 Ultra-Wideband Circular Microstrip.

This section shows the configuration of an ultra-wideband circular microstrip patch antenna device [46]. The antenna contains a circular radiator that fed by a 50 Ω. The simulation of this antenna has been done by using Ansoft high-frequency structure simulator (HFSS) and computer simulation technology- microwave studio (CST)

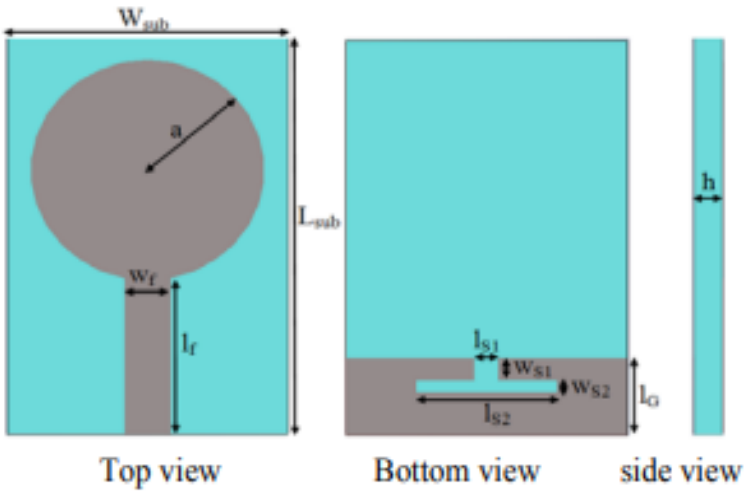

Figure 4.1 Geometry of proposed antenna [46].

The antenna, which has a compact dimension of 5mm printed on the FR-4 dielectric constant of the substrate is 4.4 and thickness 1.58 mm as shown in Figure 4.1. The partial ground plane at the bottom side of the FR-4 with the following dimensions 12×3.5 mm^2, the parameters of the printed antenna: W_{Sub}=12mm, L_{Sub}=18mm, a= 5mm, L_G = 3.5mm, i_f = 7mm, W_f = 2mm, h=1.58mm, W_{S1}= l_{S1} =1mm, l_{S2} = 6mm, W_{S2} =0.5 mm. In Figur, 4.2.(a) illustrates the reflection coefficient obtained by HFSS and CST. We have studied the same problem in [46] and obtained the result of the S_{11} by using CST 2016 version with assuming the patch thickness 0.07mm as shown in Figure 4.2.(b).

Table 4.1 Comparison of S_{11} of The Simulation Results and The Reference Results[46].

Software Package	Fmin (GHz)	Fmax (GHz)	Level S_{11}(dB)
Reference results	4.9	12.6	-16.14 -17.75
Our results	4.2	12.69	-18.85 -21.62

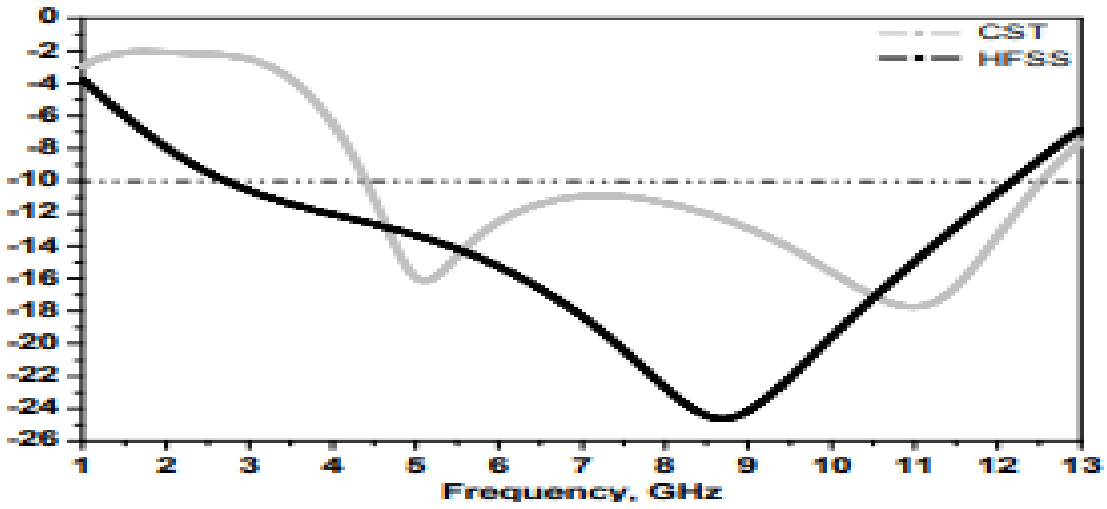

(a)

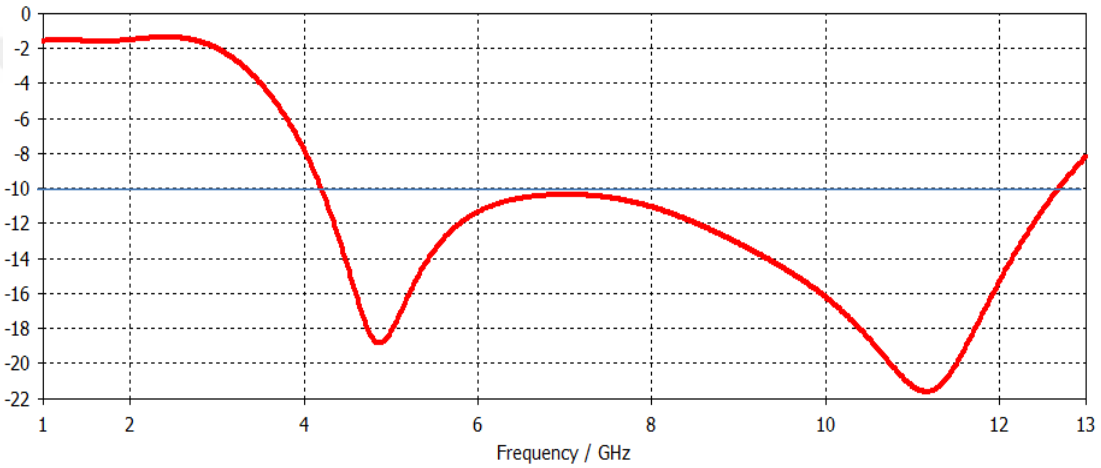

(b)

Figure 4.2 S_{11} of ultra-wideband circular microstrip (a) refernce results [47], (b) our results.

4.2.2 Novel Ultra-Wideband Antenna With Individual SRR [57]

In [57] a novel approach of small UWB antenna based on individual SRR and coupled microstrip line is used, and the operation band is from 3.6 GHz to 14.6 GHz. The shape of the antenna is as shown in Figure 4.3, the substrate is FR-4 with dielectric constant 4.2 and loss tangent 0.02, and substrate thickness 1 mm, the circular patch antenna consists of the SRR connected to feed line.

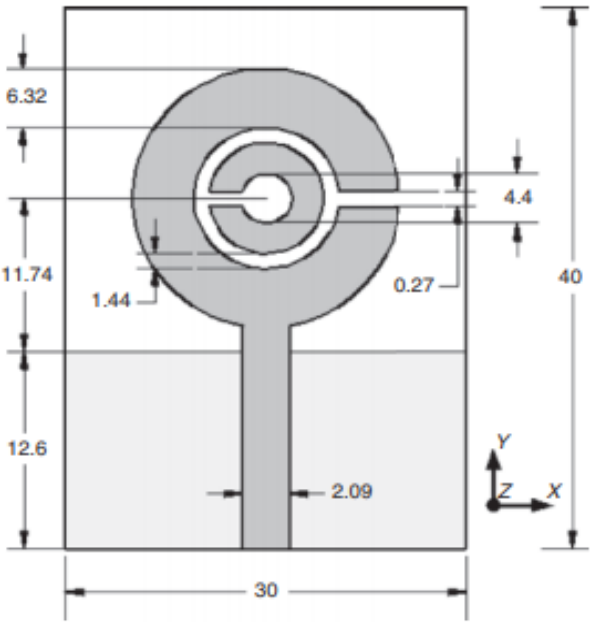

Figure 4.3 Geometry of proposed antenna [47].

From both the simulation result and the experimental results provided in [47], we can notice that the SRR can be used as a UWB antenna as shown in Figure 4.4, antenna operates beyond the whole UWB spectrum from 3.6 GHz to 14.6 GHz as seen in Figure 4.4 (a) [47].

Despite the existence of unavailable dimensions and information in the article such as a thickness of the patch and other copper parts and its position on the top of the substrate, good results were obtained after several attempts to get the frequency range starting from 2.1344 GHz to 15.7 GHz with as shown in Figure 4.4 (b). The thickness of the copper material used is taken as 0.07 mm.

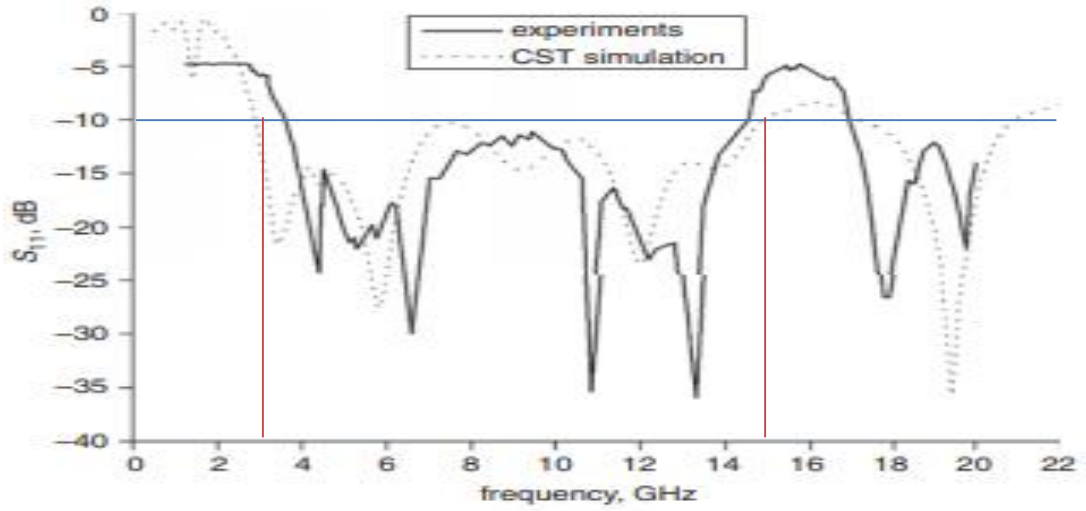

(a)

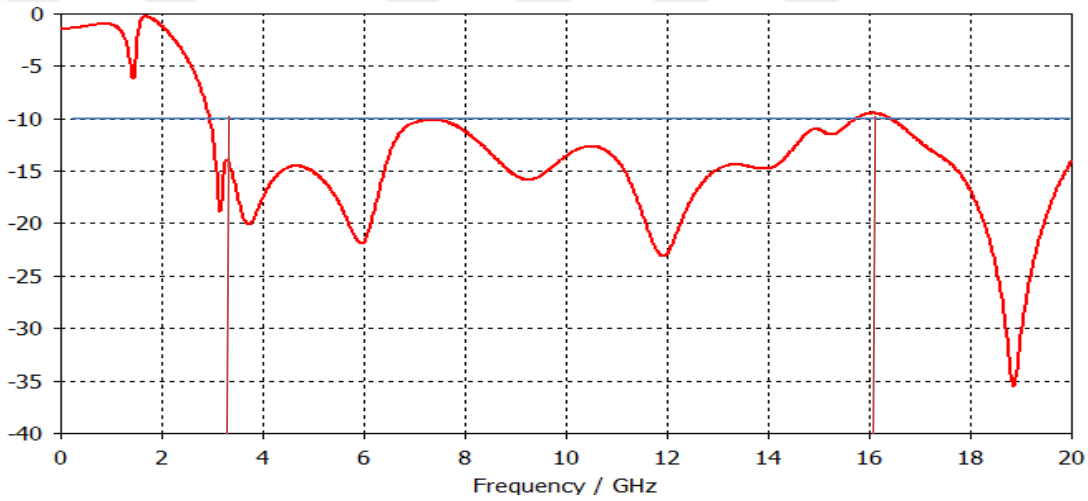

(b)

Figure 4.4 S_{11} of UWB antenna with individual SRR (a) refernce results [47], (b) our results with t=0,07.

4.3.1 Antenna Design

The proposed antenna contains three main structures, which are a patch, partial ground, and a dielectric substrate. We used the proposed antenna in chapter 3, the new substrate has been added on the top of the proposed antenna of chapter three with same material and size, the separation between the first substrate and the new one is 4 mm.

The metamaterial array located above the UWB antenna on the top of the second substrate. The proposed array consists of 2 unit cells in one row separated by distance equals to 10 mm. Both of unit cells are printed on a dielectric substrate as seen in Figure 4.5.

The single unit cell is a triple split rings resonator (TSRR) with rings with dimensions of 10×10 mm^2, 8.2 × 8.2 mm^2, and 6 × 6 mm^2. The other related dimensions in Table 4.2.

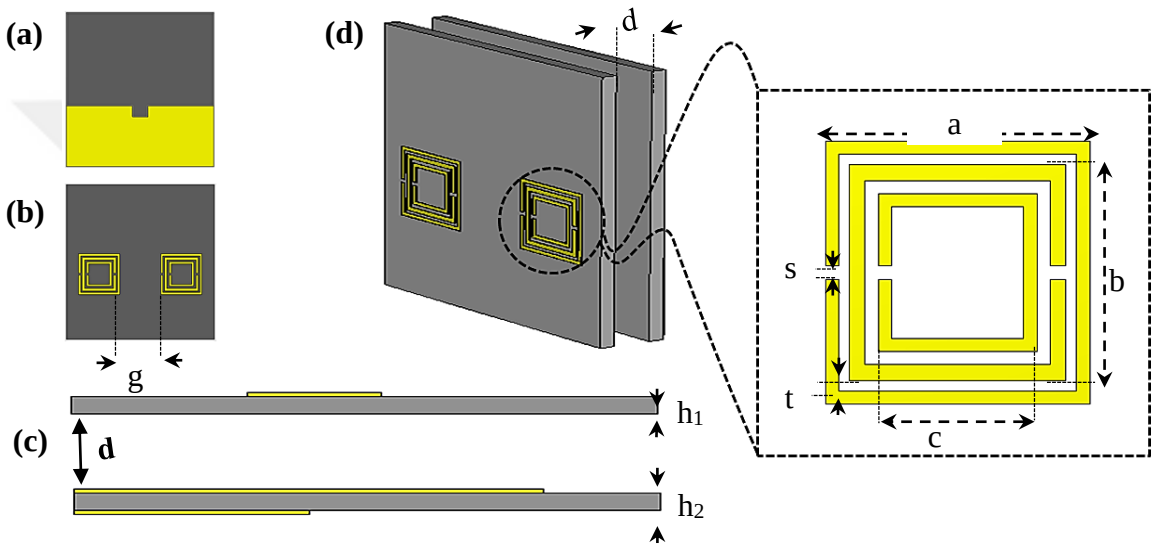

Figure 4.5 Microstrip patch antenna based on triple split rings resonator (a) back view, (b) top view, (c) side view, and (d) 3D view.

Table 4.2 Microstrip Patch Antenna Based on Triple Split Rings resonator.

Parameter	Dimensions(mm).
d	4
h_1	1.58
h_2	1.58
g	10
a	10
b	8.2
c	6
t	0.5
s	0.5

4.3.2 Result and Discussion

In this section, the performance of the antenna based MTM is discussed in terms of S_{11}, the voltage standing wave ratio (VSWR), gain, directivity.

A. S_{11} and VSWR

The performance of the antenna with the MTM structure is observed numerically in terms of S_{11} as seen in Figure 4.6. The purpose of metamaterials is to increase the gain and non-distortion of the S_{11} as shown and the nappy on the bandwidth It is found that the proposed antenna model provides a wideband of the operating frequency, from 2.6 GHz and continues beyond 20 GHz.

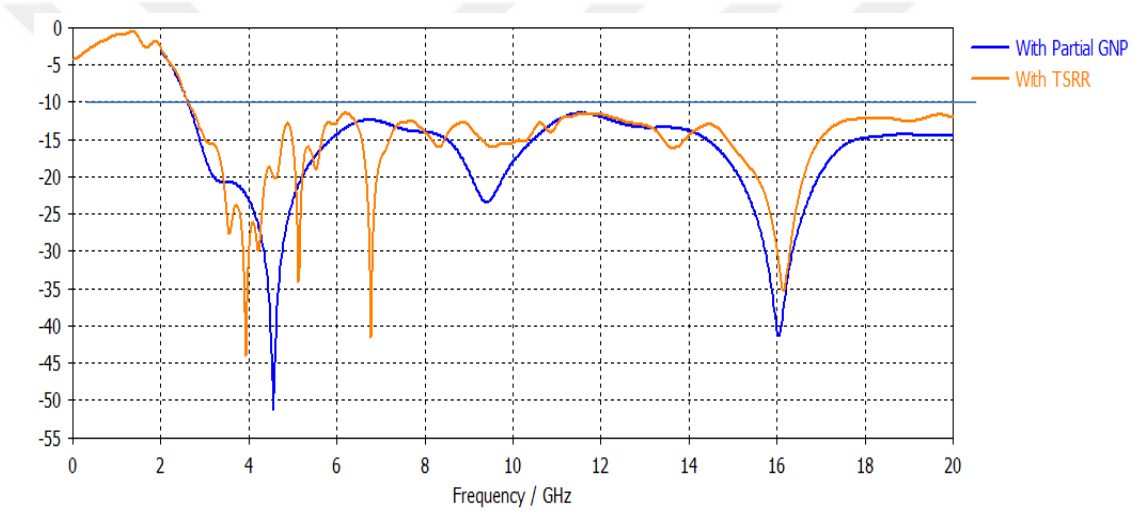

Figure 4.6 S_{11} of the microstrip antenna with TSRR and microstrip antenna with a partial ground plane.

In addition to the S_{11}, the VSWR is evaluated as seen in Figure 4.7 It's found that the antenna with TSRR structure provides a VSWR less than 2 at the frequency bands starting from 2.66 GHz and continues beyond 20 GHz.

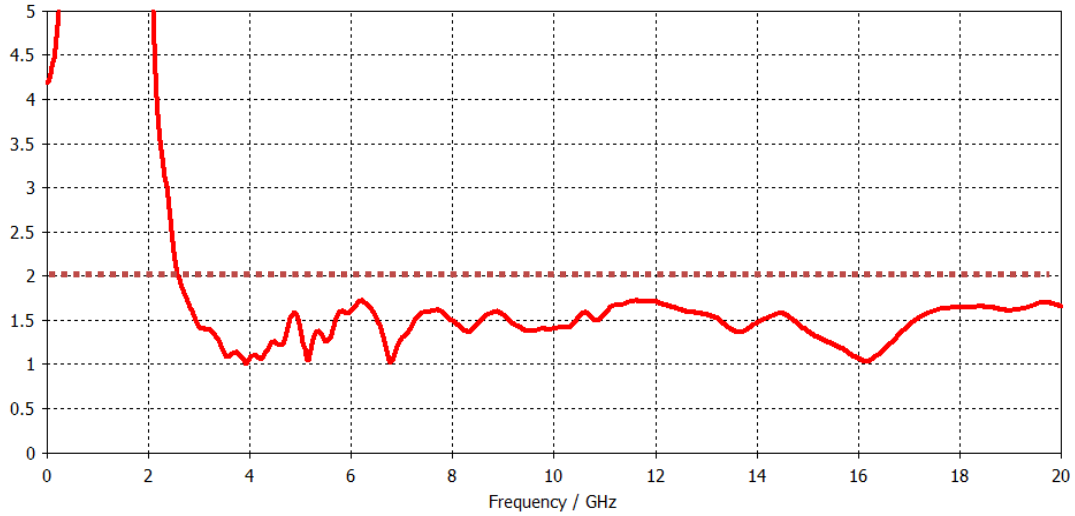

Figure 4.7 VSWR of the antenna based TSRR structures.

B. Gain

The gain of the proposed structure is evaluated and then compared with the gain of the antenna without MTM, as seen in Figure 4.8, respectively. It's found that the gain of the proposed structure antenna with TSRRs are varying from 1.36 dB to 8.13 dB at a different operating frequency, where the maximum enhancement in the gain is found equal to 3.19 dB at 16 GHz.

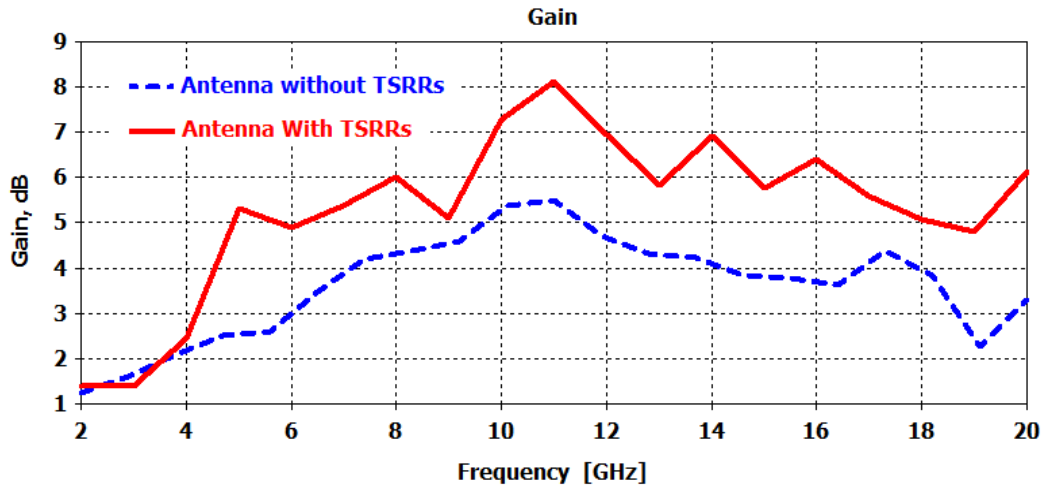

Figure 4.8 Gain a comparison between the antenna and antenna based TSRRs structures and conventional microstrip antenna.

4.4 Parametric Study

The performance of the proposed structures antenna with TSRRs would be affected by changing the geometrical dimensions of the structure. This study is conducted to find the effects of each parameter on the antenna performance. The parametric study has been followed to arrive at the optimum design is shown below:

4.4.1 UWB Antenna

A- Effect of the Substrate Thickness *h*

The effect of substrate height/thickness *h* on the S_{11} spectrum is studied by fixing the substrate length and width at 38 mm and 36 mm respectively, while *h* is changed from 1 mm up to 2 mm, with the step of 0.25 mm. In Figure 4.9, the S_{11} are shown. It's found that the antenna shows the best matching bandwidth when the thickness is 1.58 mm.

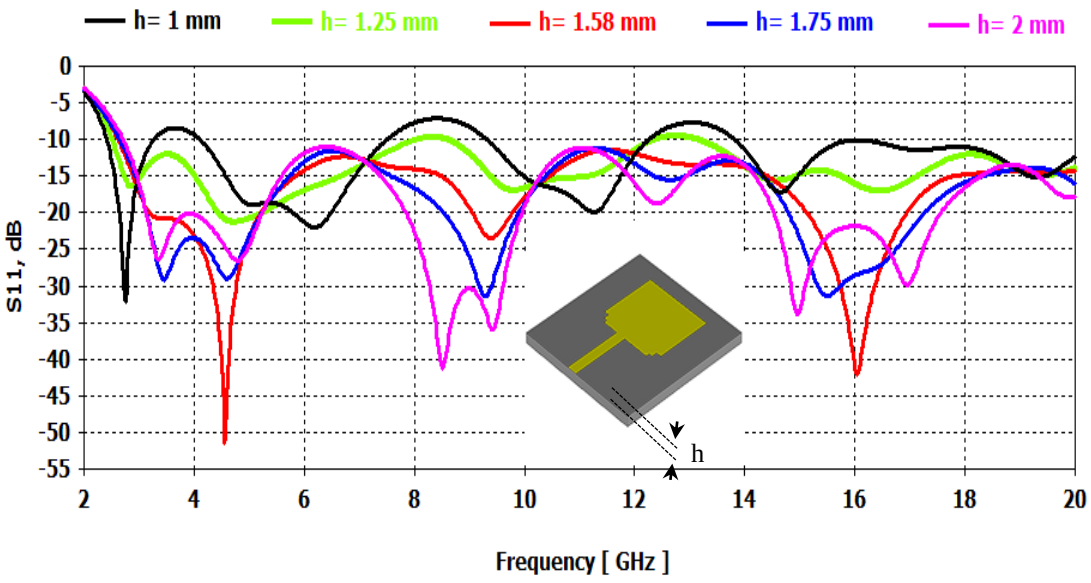

Figure 4.9 S_{11} with respect to changing h.

The reason of the antenna has the best matching at 1.58 mm thickness is back to the quality factor, where at this thickness the proposed antenna shows a lowest quality factor value compared with the other thickness and as a result, a low-quality factor means a high bandwidth due to the opposite relation between them.

B- Effect of the Ground Plane

The effect of varying the length of the ground plane is evaluated and presented in Figure 4.10. It is clear that the length of the ground (L_g) has a significant effect on the antenna performance that presented by S_{11}, which the best result is found at L_g equals to 15 mm that gives a bandwidth of 17.3418 GHz starting from 2.6582 GHz to 20 GHz.

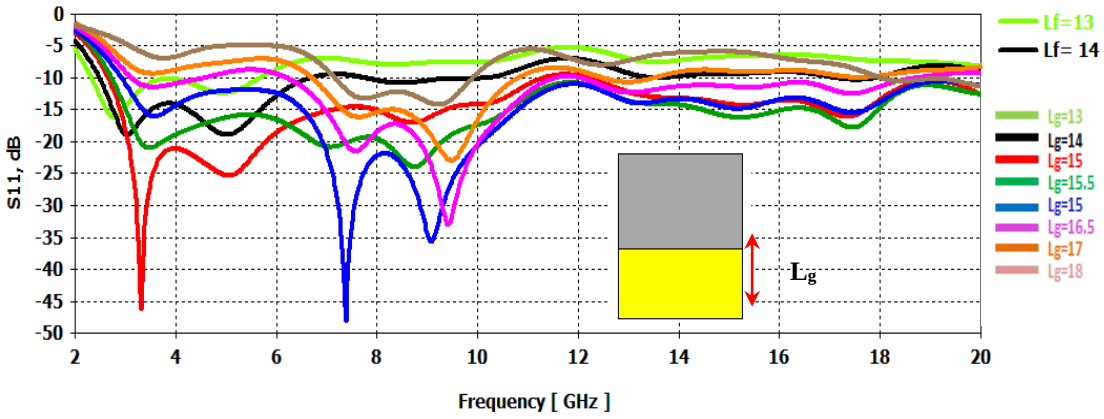

Figure 4.10 S_{11} with respect to changing L_g.

After achieving the best S_{11} with an L_g equals to 15 mm, a slot is added to the partial ground plane in order to enhance the S_{11} that have values close to -10 dB and reduce them to value below -10 dB. Figure 4.11 shows an S_{11} compression of the antenna in terms with and without a slot in the partial ground.

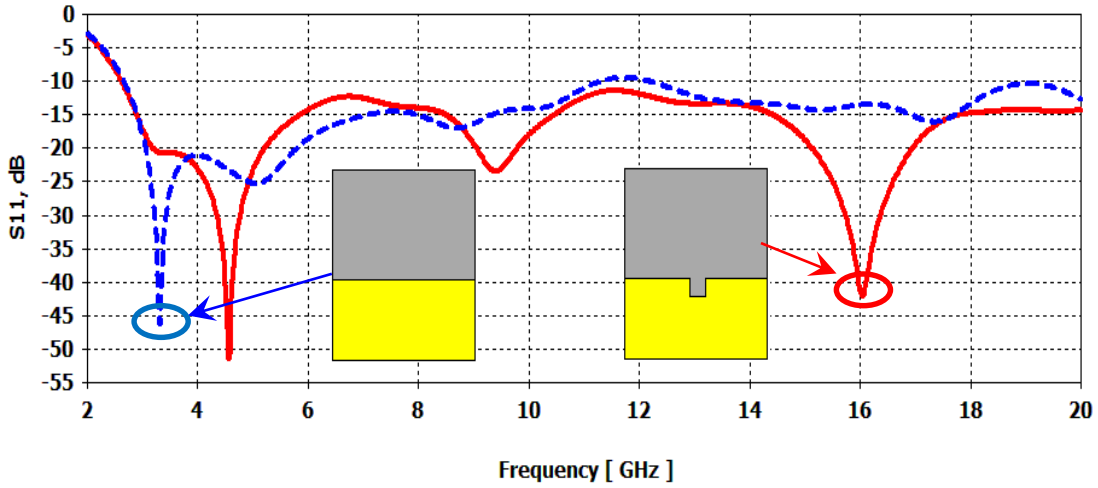

Figure 4.11 Effective of the slot on the antenna S_{11}.

4.4.2 Antenna with TSRR Structures

After completing the antenna parametric study, a new study based on TSRR structures is proposed. This study is conducted to find the effects of the TSRRs separation distance (d), a number of TSRR structures, TSRRs position, and g - gap on the antenna performance.

A- Effect of the TSRRs height *d*

In this section, the effect of the separating distance *d* as shown in Figure 4.12, on the antenna performance has been studied with considering that the optimum antenna dimensions are 38×36×1.58 mm^3.

Figures 4.13 and 4.14 show the simulated results, $S_{11,}$ and gain, of the proposed structure with multiple separating distance values. It's clear that *d* has a significant effect on the antenna performance, where the best result is found at *d* equals to 4 mm that gives a higher gain with best impedance and bandwidth.

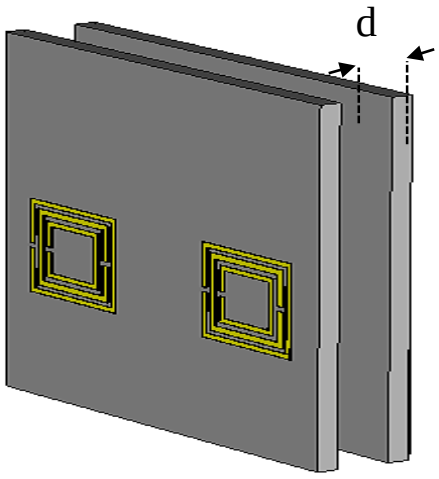

Figure 4.12 The separating distance *d* between the antenna and the TSRR array.

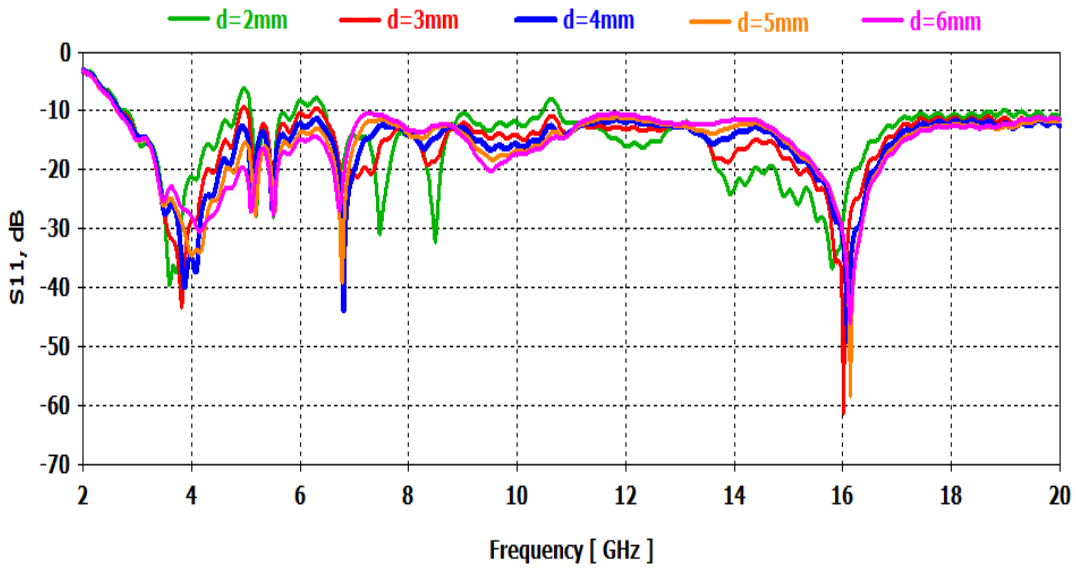

Figure 4.13 S_{11} of the multiple *d* values.

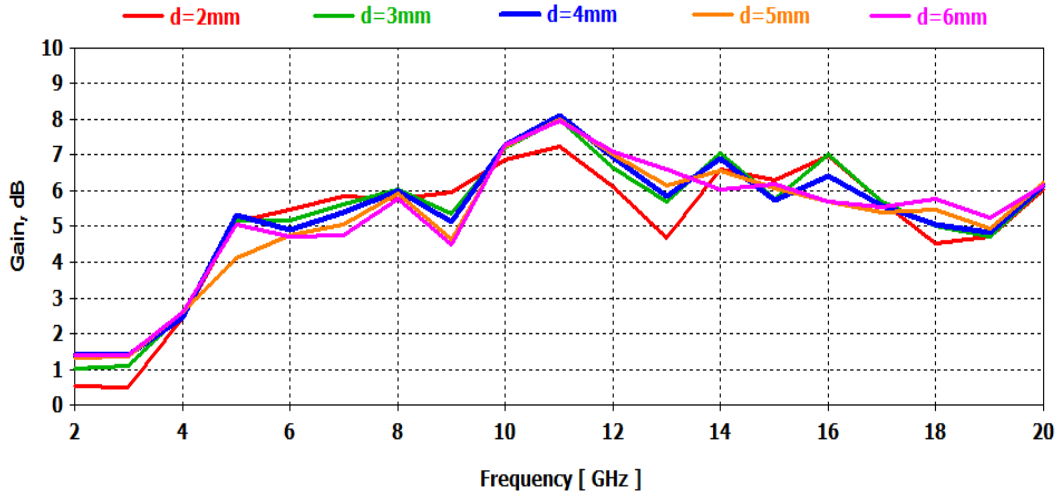

Figure 4.14 Gain of the multiple d values.

B- Effect of the TSRRs Number

The next study is presented by showing the effects of the TSRR number as shown in Figure 4.15 on the antenna performance with considering that the optimum d and antenna dimensions are equal to 4 mm and 38×36×1.58 mm^3, respectively.

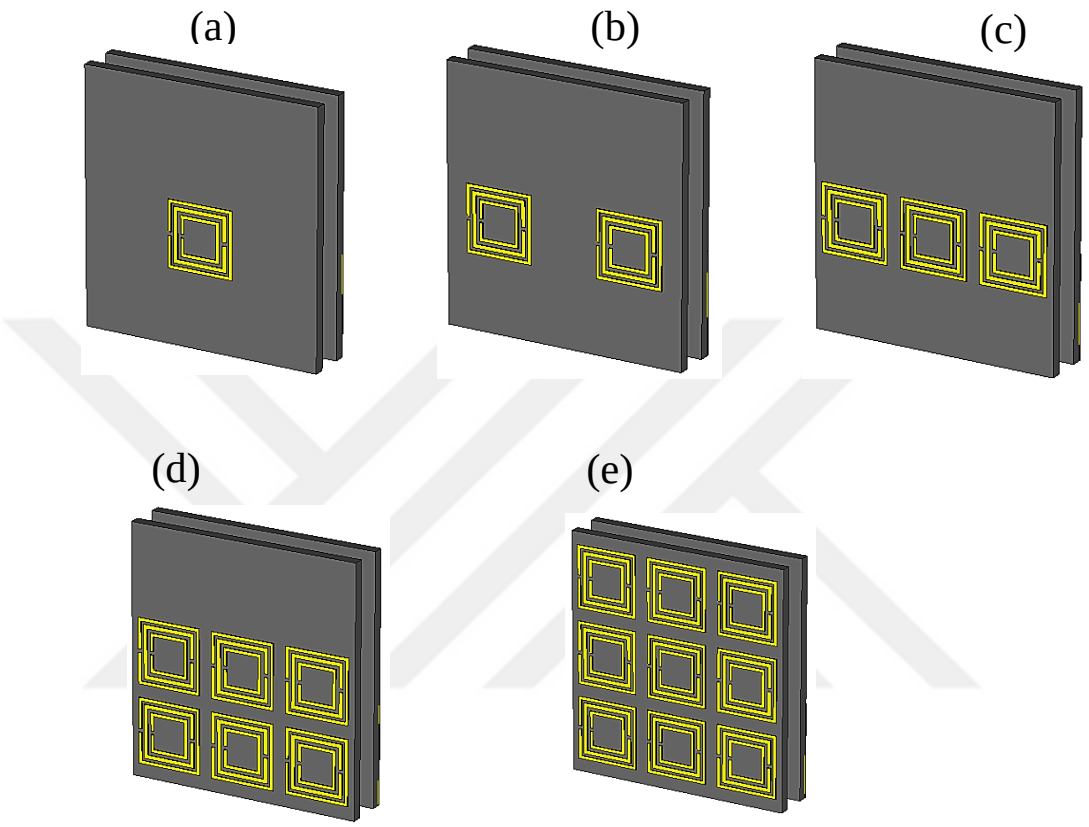

Figure 4.15 Numbers of TSRR (a) 1 TSRR, (b) 2 TSRRs, (c) 3 TSRRs, (d) 6 TSRRs, (e) 9 TSRRs.

The simulated results presented as S_{11} and gain of the different unit cell number are shown in Figures 4.16 and 4.17. It's found that the number of the unit cell has a significant effect on antenna performance. The best result is found when the array consists of two unit cells only. With this number of the unit cells, a higher gain with the best impedance bandwidth is obtained.

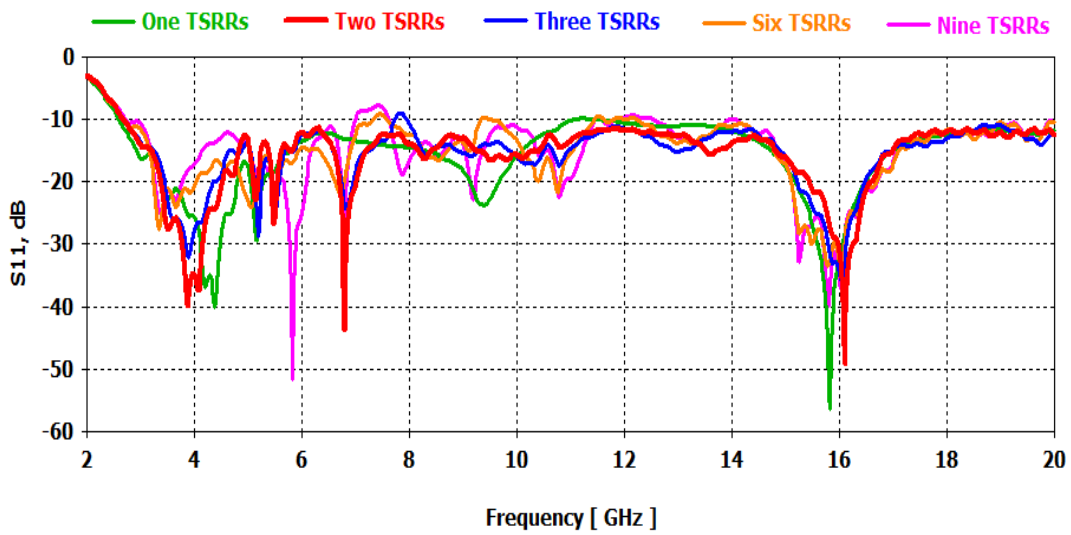

Figure 4.16 S_{11} of the different unit cell number.

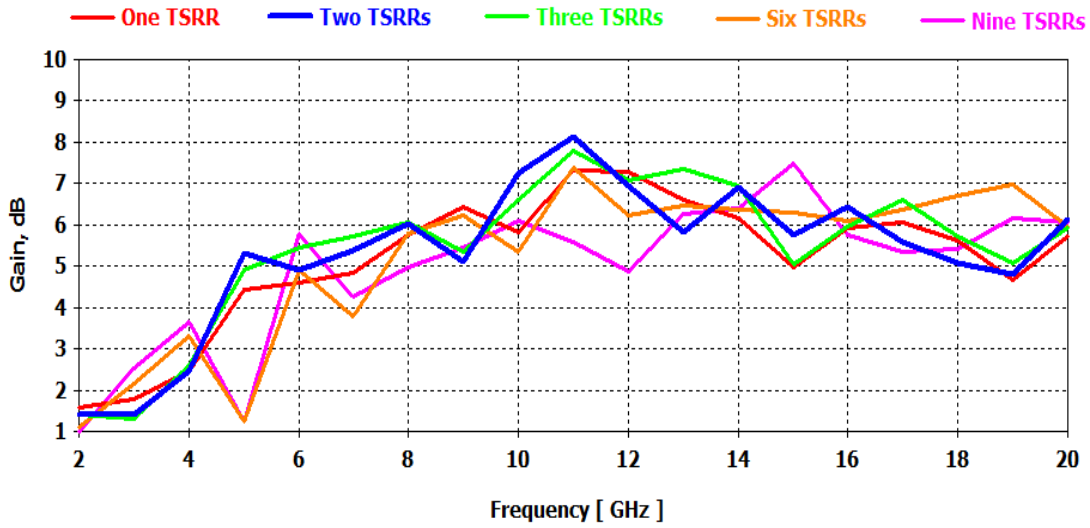

Figure 4.17 Gain of the different unit cell number.

C- Effect of the TSRRs Position

In addition to all previous studies, a new study based on the best TSRR unit cells position has been presented in this section. This study is focusing on finding the best TSRR position that gives higher gain with the best impedance bandwidth.

As shown in Figure 4.18, many positions have been chosen to study taking into consideration that the optimum *d* value, antenna dimensions, and the number of the unit cell are equal to 4 mm, 38×36×1.58 mm^3, and 2 TSRRs, respectively.

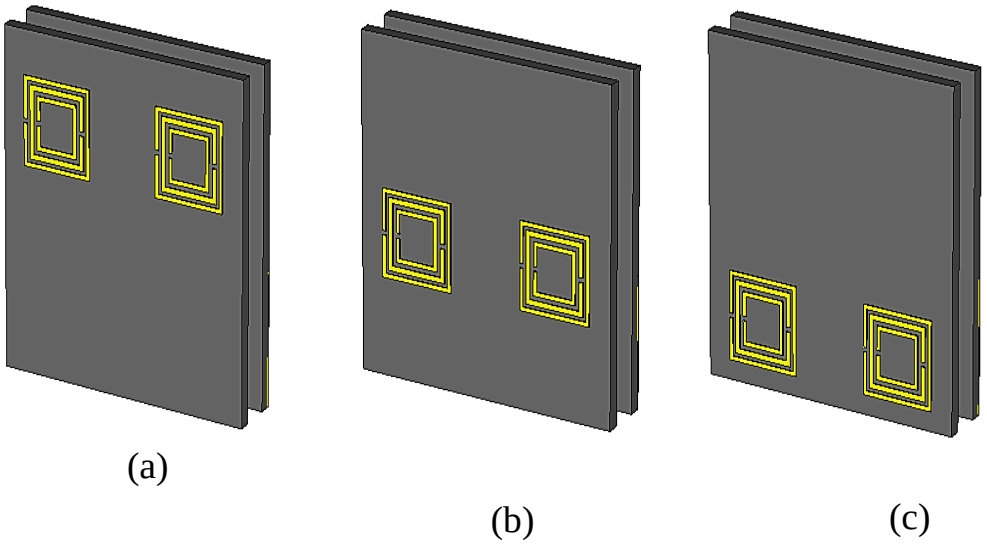

Figure 4.18 Different TSRR positions (a) upper position, (b) central position, (c), lower position.

For all TSRRs positions, the structure performance presented by S_{11} and gain is found as shown in Figures 4.19 and 4.20. From the obtained results, it's clear that the unit cells position can effect on the antenna performance. It's found that a higher gain with the best impedance bandwidth, is achieved when the unit cells are located in the center.

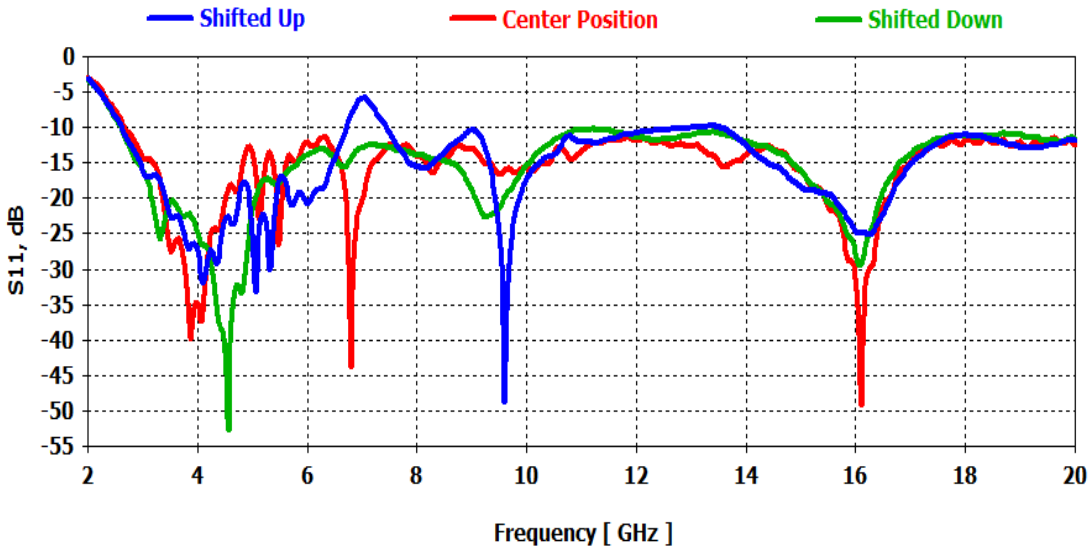

Figures 4.19 S_{11} of the different unit cells positions.

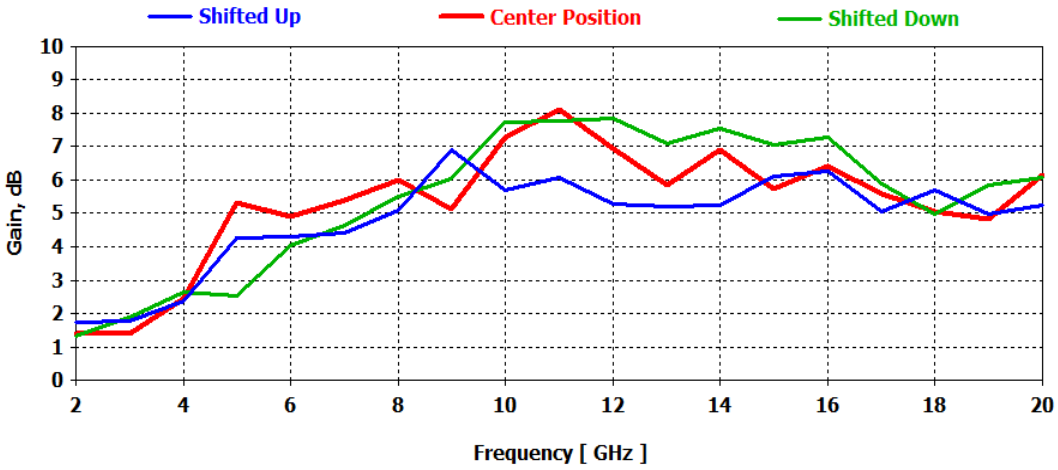

Figures 4.20 Gain of the different unit cells positions.

D- Effect of the g - gap

The last parameter that has been studied the effect of it on the antenna performance is the g – gap that saw in Figure 4.21. This work is focusing on finding the optimum g-gap value that gives the best result with considering that the optimum *d*, antenna dimensions, and a number of the unit cells with their position are equal to 4 mm, 38×36×1.58 mm^3, and 2 TSRRs in the center, respectively.

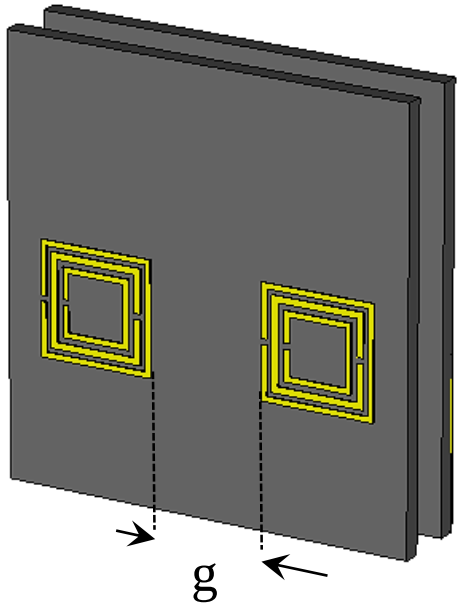

Figure 4.21 g – the gap between the two TSRR unit cells.

Figure 4.23 and Figure 4.24 shows the simulated results, $S_{11,}$ and gain, of the proposed structure with multiple g-gap values. It's clear from the obtained result that the gap has not a significant effect on the antenna performance, we chose that 10 mm because of ripples in case 10 mm less than others and the stability of the S_{11} under -10 dB.

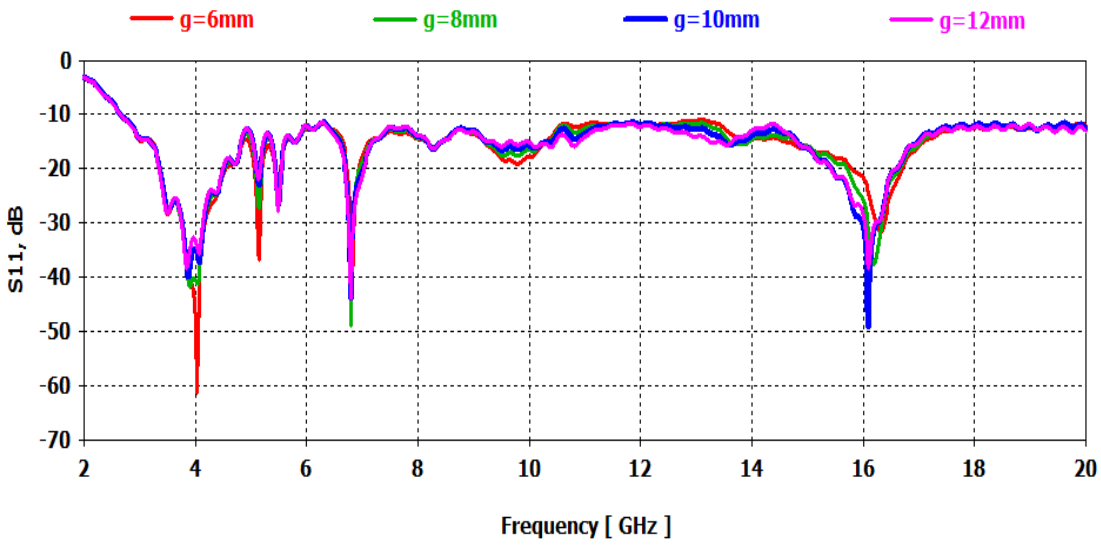

Figure 4.22 S_{11} of the multiple g - gap values.

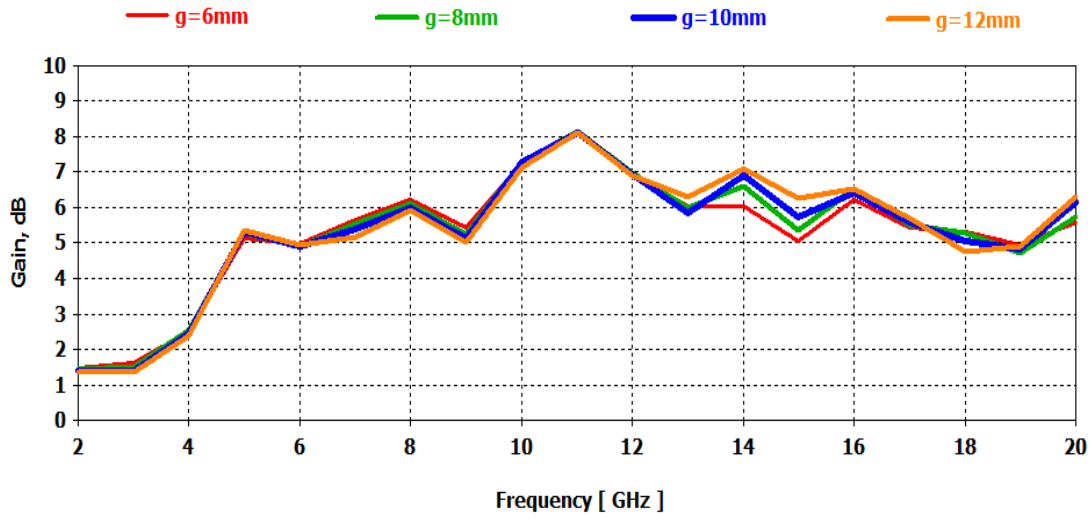

Figure 4.23 Gain of the multiple g - gap values.

4.5 Circular Patch Antenna

In attempt to increased antenna performance of the proposed antenna [46], the proposed structure design geometry is consisting of two main parts UWB circular

microstrip patch antenna and partial ground plane with same material and size, we have added a slot that starts from the center of the patch cross to the transmission line seen in Figure 4.24. other dimensions and parameters mentioned in section 4.2.1.

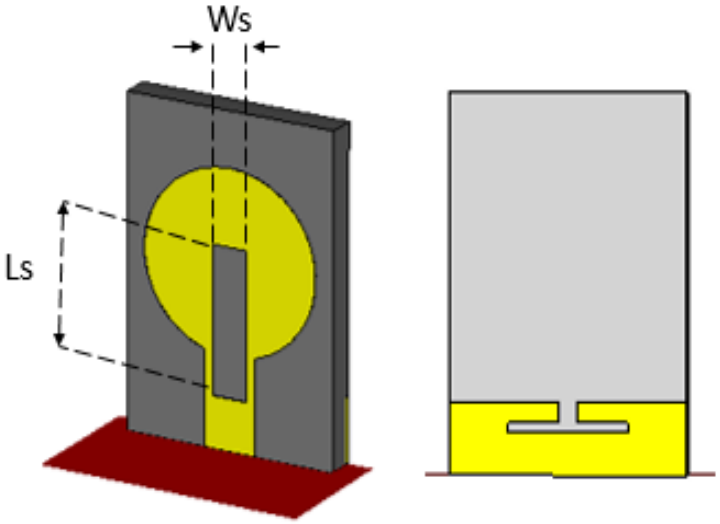

Figure 4.24 Circular patch antenna with central slot (a) front view, (b) back view

.

Table 4.3 Circular Patch Antenna with Central Slot.

Parameter	Dimensions(mm)
Ws	2
Ls	8

The performance of the antenna with a slot is observed numerically in terms of S_{11} as seen in Figure 4.25 and the VSWR in Figure 4.26. It is found that the proposed antenna model provides a wideband of the operating frequency from 4.55 GHz to 13.5 GHz. The comparison of the results between our results and the proposed as shown in Figure 4.32, S_{11} enhanced about 1.4 GHz as is it in the VSWR as seen in Figure.4.33.

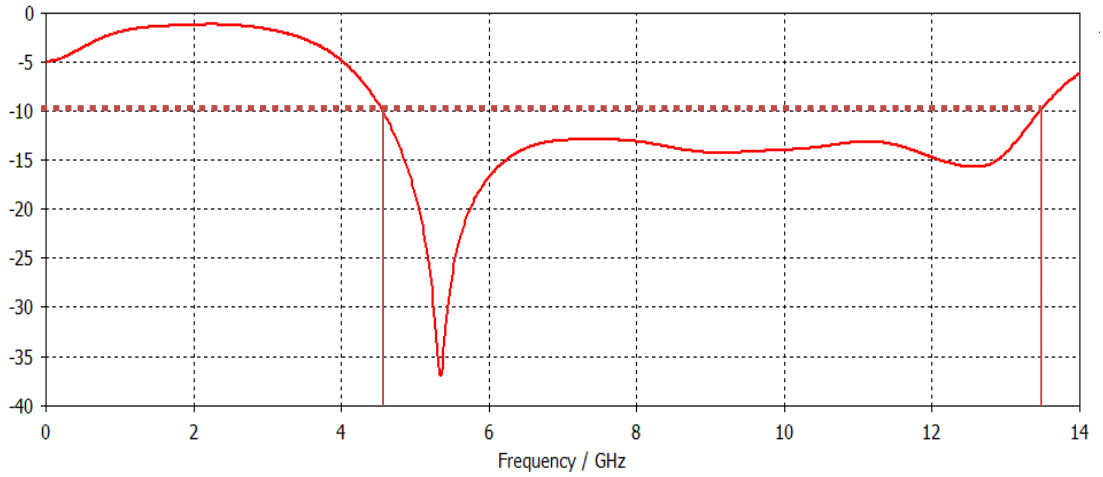

Figure 4.25 S_{11} circular patch antenna with the central slot.

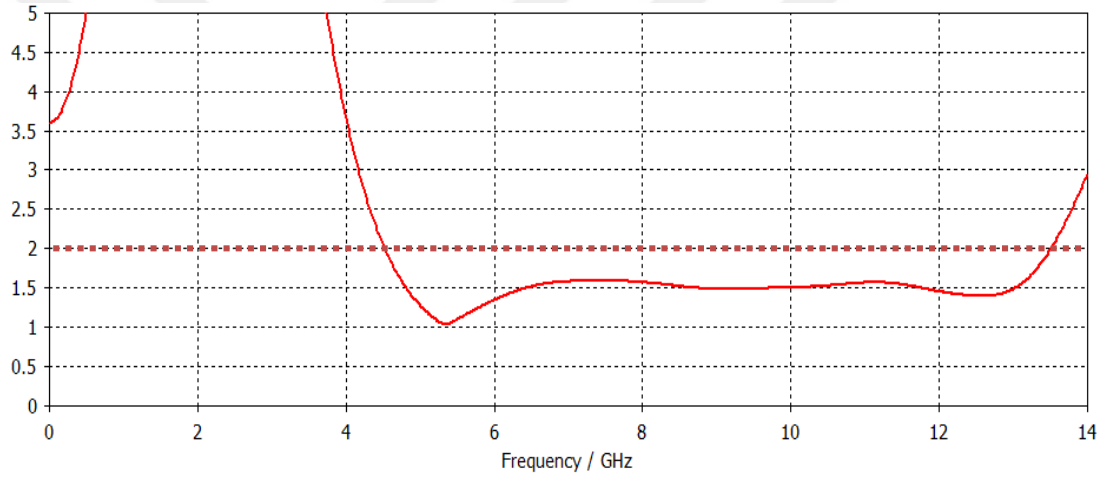

Figure 4.26 VSWR of the circular patch antenna with the central slot.

4.6 CST vs. HFSS Results

A. HFSS

HFFS is considered to be one of the tools that have found extensive usage in industrial design environments. HFSS aims to obtain parasitic parameters (S, Y, Z), and therefore visualize a three-dimensional electromagnetic field (near and far field) so that SPICE models can be generated. These processes are all based on the 3D FEM solution of the electromagnetic topology being considered. One of HFSS' most useful attributes is its ability to automatically generate an adaptive mesh, which in the majority of cases

works by editing the concern of the designer about the grid of your choice. This is a very common program and is utilized for all types of purposes [48]. It is generally able to predict input impedance and radiation patterns very well. However, there are not a lot of results about the efficiency.

B. CST

The basis of CST microwave studio (CST MWS) is the finite integration technique (FIT). There is an option to assign the simulator as either a time domain or frequency domain, despite the fact that eigenmode, transient, and frequency domain solvers are found in CST MWS [48] Time domain solver computes the electromagnetic devices' broadband behavior during the operation of a single simulation having an arbitrary accurate frequency accuracy. The automatic mesh generator is able to identify the significant points within the structure (fixpoints) and find the mesh nodes within it. The user also has the ability to manually add fixpoints on the structure, as well as gain full control of the number of mesh lines for every coordinate in terms of the specific wavelength. Power-based mesh adaptability makes it possible to implement improvements in a predetermined amount of passes, offering a consistent improvement within the advanced design features even if a longer simulation time is spent. , has garnered much popularity over the past several years.

D. UWB antenna design using the different simulator

This difference can be a result of the various modeling of the feed. for both CST MWS and HFSS, which means that both the simulators are different because they have varying computational techniques involved. HFSS results bear proximity to experimental results and possess more insight into the available structure. To illustrate the above, you will simulate UWB antennas and study methods for earlier projects (microstrip patch antenna and circular patch antenna). The microstrip return loss for patch antenna based on double TSRR calculated in between 2 GHz and 20 GHz as shown in Figure. 4.27, Figure 4.28.

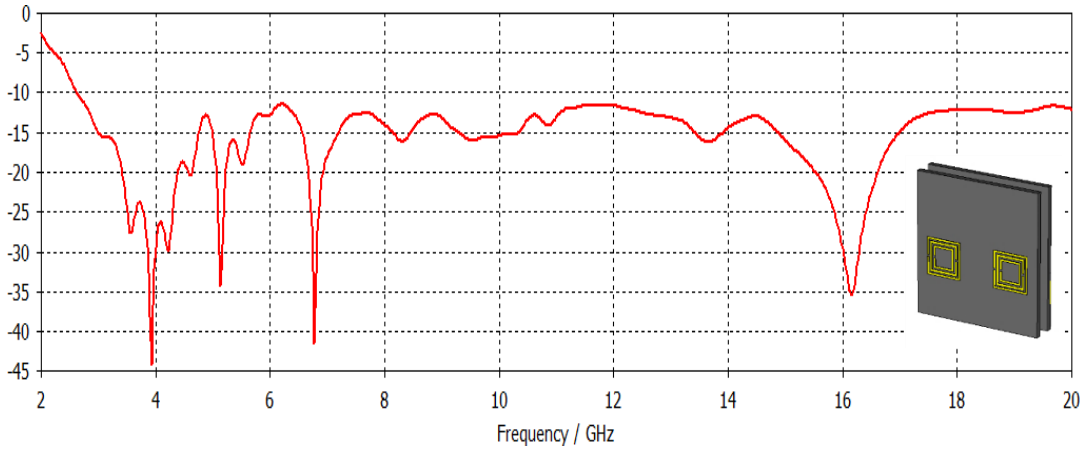

Figure 4.27 Simulation UWB microstrip patch antenna using CST.

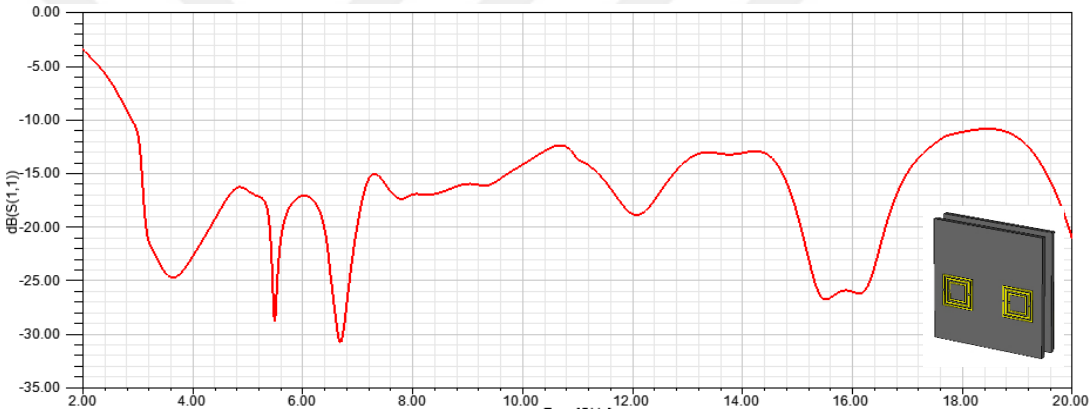

Figure 4.28 Simulation UWB microstrip patch antenna using HFSS.

Table 4.4 Nominal Frequency Values for UWB Antenna with TSRR.

Software Package	Fmin (GHz)	Fmax (GHz)
CST MWS	2.66	20
HFSS	2.135	20

The operating frequency of simulation results in Figure 28 an Figure 29 show S_{11} from 2 GHz to 20 GHz. The difference between Fmin and Fmax represents the bandwidth (BW). The return loss for the circular patch antenna with slot simulated in between 2 GHz and 14 GHz is presented in Figure. 4.29, Figure 4.30.

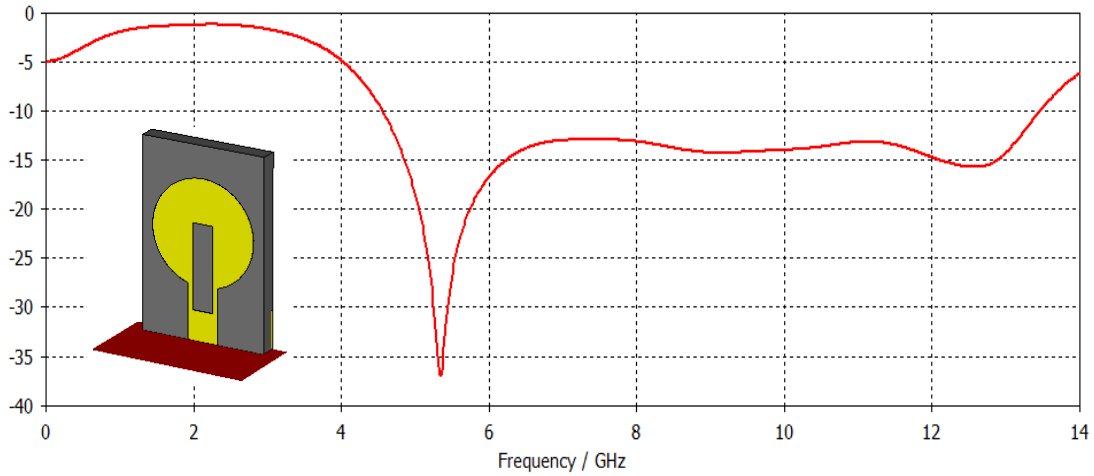

Figure 4.29 Simulation and results for UWB circular patch antenna using CST.

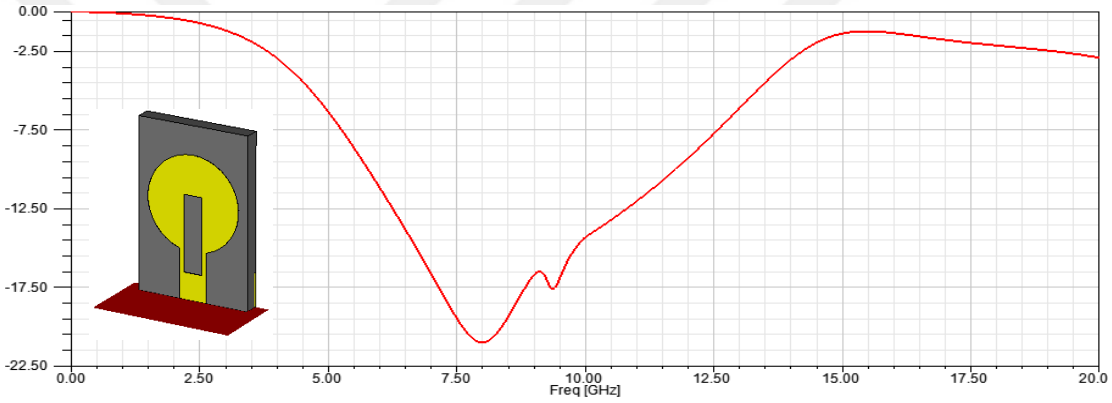

Figure 4.30 Simulation and results for UWB circular patch antenna using HFSS.

Table 4.5 Nominal Frequency Values for UWB Circular patch Antenna.

Software Package	Fmin (GHz)	Fmax (GHz)
CST MWS	4.45	13.4
HFSS	5.8	12

CHAPTER 5

CONCLUSIONS AND SUGGESTIONS FOR FUTURE WORK

5.1 Conclusions

In this study, the antenna design with metamaterial structure geometry is proposed. The performance of the proposed antenna with and without MTM structures is validated. A systematic approach based on the parametric study is applied to arrive at the best structure performance; nevertheless, the same approach is applied to obtain the antenna dimensions for the maximum bandwidth and gain. The most important realized achievements can be summarized in the following list:

1. UWB antenna with TSRR is introduced, as compared to the traditional design; this design has a compact configuration, a wide bandwidth, and a higher gain.
2. Comparing the proposed UWB antenna with respect to the traditional microstrip patch antenna, the proposed UWB antenna characterized by wider bandwidth due to a transition steps and a partial ground plane with a slot.
3. Adding the metamaterial structures to the UWB antenna design improved the Gain of about 3.19 dB.

5.2 Suggestions for Future Work

Future work involves the following suggestions:

4. Use another type of feeder technique and compare the results with that presented in our work.
5. Adding extra MTM type such as zero indexes / electromagnetic bandgap MTM at the front of the antenna for more gain enhancement.

6. Applying the active component to the metamaterial structure to obtain reconfigurable characteristics then apply this to the antenna for reconfiguring the performance.
7. Using an antenna array for steering the radiation over the frequency range of interest.
8. Developing the planner array to the folded, cylindrical and conical antenna shapes.
9. Developing an embedded metamaterial structure with negative constitutive parameters inside the substrate of the antenna to enhance the antenna.

REFERENCES

[1] K. M. Luk, C. L.Mak, Y. L. Chow and K. F. Lee, July 1998, "Broadband Microstrip Patch Antenna," Electronics Letters, **vol. 34,** no. 15, pp. 1442-1443.

[2] Vijay Sharma, Rajesh Sharma, V K Saxena, Deepak Bhatnagar, and V S Kulhar Krishan Gopal Jangid, October 2015, "Design of Compact Microstrip Patch Antenna with DGS Structure for WLAN & Wi-MAX Applications," European Journal of Advances in Engineering and Technology, **vol. 2**, no. 1, pp. 8-11.

[3] S. H. Author et al August 2003, "A New Ultra Wide Band antenna for UWB application", Department of Radio Wave Engineering Hanbat National University.

[4] K.-S. Author et al, 2008, Design, and construction of microstrip UWB antenna with time domain analysis.

[5]S. H. Author et al, August 2003, "A New Ultra Wide Band antenna for UWB application", Department of Radio Wave Engineering Hanbat National University.

[6] M.G. Author and M. Y. Writer, January 2012, Bandwidth Enhancement Techniques Comparison for Ultra Wideband Microstrip Antennas for Wireless Application " in Journal of Theoretical and Applied Information Technology.

[7] Debashish Pal, October 2014, "Design of a Novel Triangular Shaped Fractal Antenna for Wireless Communication," SSRG International Journal of Electronics and Communication Engineering (SSRG-IJECE), **vol. 1**, no. 8, pp. 25-28.

[8] Swapnil M. Vanam, Prof. R. P. Labade, May-June 2014, "Parametric Analysis and Design of Rectangular Microstrip Patch Antenna for Ultra-wideband Application," International Journal of Microwaves Applications, **vol. 3**, no. 3, pp. 17-20.

[9] Sajith, K., Gandhimohan, J., & Shanmuganantham, T. (2017). Design of SRR loaded octagonal slot CPW fed wearable antenna for EEG monitoring applications. 2017 IEEE International Conference on Circuits and Systems (ICCS).

[10] Ridha S., M. Labidi, and F. Choubani, December 2015, “A coplanar wideband antenna based on metamaterial refractive surface,” Applied Physics A Materials Science and Processing, Springer, **Vol. 122**, No. 1.

[11] Kurra, L., M.P. Abegaonkar, A. Basu, and S.K. Koul, January 2016, “ FSS properties of a Uni-planar EBG and its Application in Directivity Enhancement of a Microstrip Antenna,” IEEE Antennas and Wireless Propagation Letters, No. 99, PP. 1- 5.

[12] Robert Vilaltella Esteve, 2013, "High-Efficiency Dual-Polarized Patch Antenna Array with Common Waveguide Feed," Universitat Stuttgart, thesis.

[13] Nasimuddin, Microstrip Antennas. India: Intech publisher, 2011.

[14] Robert Vilaltella Esteve, 2013, "High-Efficiency Dual-Polarized Patch Antenna Array with Common Waveguide Feed,".

[14] A.Sainati, Robert, 1996, CAD of Microstrip Antenna for Wireless Applications.: Artech House.

[15] R. B. Waterhouse, 2003, Microstrip Patch Antennas: A Designer's Guide. New York: Springer Science and Business Media.

[16] Dana Saeed Muhammad, 2007, "Bandwidth Improvement and Size Reduction of Microstrip Patch Antenna using HFFS," University of Sulaimani, Sulaimani.

[17] Soumya Ranjan Behera, 2010, "Dual Band and Dual Polarized Microstrip Patch Antenna," National Institute of Technology Rourkela, India.

[18] J R James & P S Hall, 1989, Hand Book of Microstrip Antennas. London, united kingdom: IEE Electromagnetic Waves Series 28.

[19] Thomas A. Milligan, 2005, Modern Antenna Design, 2nd ed. Hoboken, New Jersey: John Wily & Sons.

[20] Keith R. Carver & James. W Mink, January 1981, "Microstrip Antenna Technology," IEEE Transactions on Antenna and Propagation, **vol. 29**.

[21] Constantine A. Balanis, Antenna Theory Analysis and Design, John Wiley & Sons, Inc., 111 River Street, Hoboken, NJ 07030.

[22] G. Quintero, J.F. Zürcher, 2016 and A.K. Skrivervik, System Fidelity Factor: A new method for comparing UWB antennas, IEEE Transactions on Antennas and Propagation.

[23] Patil V. P., October 2012, "Enhancement of Bandwidth of Rectangular Patch Antenna Using Two Square Slots Techniques," International Journal of Engineering Sciences & Emerging Technologies.

[24] Constantine A. Balanis, Antenna Theory Analysis and Design, John Wiley & Sons, Inc., 111 River Street, Hoboken, NJ 07030.

[25] Prakash, P., Abegaonkar, M. P., Basu, A., & Koul, S. K. (2013). Gain Enhancement of a CPW-Fed Monopole Antenna Using Polarization-Insensitive AMC Structure. IEEE Antennas and Wireless Propagation Letters, **vol. 12**, 1315–1318.

[26] Sharifian Mazraeh Mollaei, M., Zanganeh, E., & Feshki Farahani, M., 2017, Enhancement of Patch Antenna Gain Using Cylindrical Shell-Shaped Superstrate. IEEE Antennas and Wireless Propagation Letters, **vol. 16**, 2570–2573.

[27] Vivekananda Lanka Subrahmanya, 2009, "The Rectangular Microstrip Patch Antenna," Boras, Swedish.

[28] C. Vishnu Vardhana Reddy, 2009, "Design of Linearly Polarized Rectangular Microstrip Patch Antenna using IE3D/PSO," Rourkela Deemed university.

[29] Z. N. Chen and M. Y. W. Chia, 2006, Broadband Planar Antennas Design and Applications. England: John Wiley & Sons.

[30] Yahya Entiefa Mansour, 2014, "Single Slot Dual Band Microstrip Antenna for WiMAX Application," Atilim University.

[31] Ahmed Fatthi Alsager, 2011, "Design and Analysis of Microstrip Patch Antenna Arrays," Borås University, Sweden.

[32] C. Vishnu Vardhana Reddy, 2009, "Design of Linearly Polarized Rectangular Microstrip Patch Antenna using IE3D/PSO," Rourkela Deemed university.

[33] S. Humphries and Jr. Albuquerque, 2010, Finite Element Method in Electromagnetics. USA, New Mexico.

[34] S. M. Shum and K. M. Luk, March 1998, "FDTD Analysis of Probe-fed Cylindrical Dielectric Resonator Antenna," IEEE Transactions on Antenna & Propagation, **vol. 46**, no. 3, pp. 325-333.

[35]Nader Engheta and Richard W. Ziolkowski, " Metamaterials Physics and Engineering Explorations ", 1st edition: Wiley Interscience-IEEE Press, July 11, 2006.

[36]Christophe Caloz and Tatsuo Itoh, November 25, 2005., "Electromagnetic Metamaterials: Transmission Line Theory and Microwave Applications ", 1st edition: Wiley Interscience

[37]Benedikt A. Munk, February 24, 2009, "Metamaterials: Critique and Alternatives", 1st edition: Wiley Interscience.

[38]Viktor G Veselago, Jan-Feb 1968, "The electrodynamics of substances with simultaneously negative values of ε and μ," Soviet Physics Uspekhi, **vol. 10**, no. 4, pp. 509-514.

[39]J. B. Pendry, A. J. Holden, June 1996, W. J. Stewart and I. Youngs, "Extremely Low-Frequency Plasmons in Metallic Mesostructures," Physical Review Letters, APS Physics, **vol. 76**, no. 25, pp. 1 - 12.

[40] JB Pendry, A J Holden, Feb. 1999, D J Robbins and W J Stewart, "Low-Frequency Plasmons in Thin Wire Structures," Journal of Physics: Condensed Matter, IOP Science, **vol. 10**, no. 22, pp. 1 – 31.

[41] David Smith, Sheldon Schultz, Norman Kroll, and Richard A.Shelby, sep. 14, 2004, "Left Handed Composite Media," Patent, US 6,791,432 B2.

[42] D. R. Smith, Willie J. Padilla, D. C. Vier, S. C. Nemat-Nasser and S. Schultz, "Composite Medium with Simultaneously Negative Permeability and Permittivity," Physical Review Letters, APS Physics, **vol. 84**, no. 18, pp. 4184 - 4187, MAY 2000.

[43] R. A. Shelby, D. R. Smith and S. Schultz, 6 Apr. 2001, "Experimental Verification of a Negative Index of Refraction," Science, American Association for the Advancement of Science (AAAS), **vol. 292**, no. 5514, pp. 77-79.

[44] Darshansinh N. Patel, Mohammed G. Vayada and Vimal H. Nayak, "Improvement in Characteristics of Microstrip Antenna with the Help of Different.

[45] Meta material Structures, November 2014," International Journal for Innovative Research in Science & Technology (IJIRST), **vol. 1**, no. 6, pp. 244-248.

[46] Soufian Lakrit and Hassan Ammor, March 2015, "Design Of Ultra Wideband Small Circular Patch Antenna fo Wireless communication" ARPN Journal of Engineering and Applied Sciences, **vol. 10,** no. 4.

[47] Yang, X., Yu, Z., Shi, Q., & Tao, R., 2008. Design of novel ultra-wideband antenna with individual SRR. Electronics Letters, **vol. 44** no. 19.

[48] A Practical Guide to 3D Electromagnetic Software Tools Guy A. E. Vandenbosch and Alexander Vasylchenko1.

[49] A Review, Harmandeep Kaur, Aditi Sharma, 6 June 2017, Microstrip Patch Antennas using Metamaterials, Volume 6.

[50] A. Bakhtiari, R. A. Sadeghzadeh & M. Naser. Moghadasi, 26 Mar 2018, Gain Enhanced Miniaturized Microstrip Patch Antenna Using Metamaterial Superstrates, ISSN: 0377-2063, pp.

[51]Abdullah, N., Bhardwaj, G., & Sunita, 2017. Design of squared shape SRR metamaterial by using rectangular microstrip patch antenna at 2.85 GHz.

[52]Ajay, V. G., & Mathew, T. 2017. Size reduction of microstrip patch antenna through a metamaterial approach for WiMAX application.

[53] Bhat, P. S., Kashyap, P. C., & Naik, S. 2018. Mutual Coupling Reduction Using Double Negative Metamaterial Based Dual-Line Split-Ring Resonator (DLSRR) Arrays in Microstrip Patch Antenna Arrays for L-Band and X-Band Applications.

[54] Jansri, C., Phongcharoenpanich, C., & Lamultree, S. 2018. A Printed Circular Monopole Antenna with Slot and Modified Ground Plane for UWB Applications.

[55] Xavier, G. V. R., da Costa, E. G., Serres, A. J. R., Nobrega, L. A. M. M., Oliveira, A. C., & Sousa, H. F. S. 2019. Design and Application of a Circular Printed Monopol Antenna in Partial Discharge Detection.